2022

Recent advances in biosensors for detection of COVID-19 and other viruses

Shobhit K. Patel

Jaymit Surve

Juveriya Parmar

Kawsar Ahmed

Francis M. Bui

See next page for additional authors

Authors

Shobhit K. Patel, Jaymit Surve, Juveriya Parmar, Kawsar Ahmed, Francis M. Bui, and Fahad Ahmed Al-Zahrani

Published (2022) in IEEE Reviews in Biomedical Engineering

Recent advances in biosensors for detection of COVID-19 and other viruses

Shobhit K. Patel, *Senior Member, IEEE*, Jaymit Surve, *Graduate Student Member, IEEE*, Juveriya Parmar, *Graduate Student Member, IEEE*, Kawsar Ahmed, *Graduate Student Member, IEEE*, Francis M. Bui, *Member, IEEE* and Fahad Ahmed Al-Zahrani

***Abstract*— This century has introduced very deadly, dangerous, and infectious diseases to humankind such as the influenza virus, Ebola virus, Zika virus, and the most infectious SARS-CoV-2 commonly known as COVID-19 and have caused epidemics and pandemics across the globe. For some of these diseases, proper medications, and vaccinations are missing and the early detection of these viruses will be critical to saving the patients. And even the vaccines are available for COVID-19, the new variants of COVID-19 such as Delta, and Omicron are spreading at large. The available virus detection techniques take a long time, are costly, and complex and some of them generates false negative or false positive that might cost patients their lives. The biosensor technique is one of the best qualified to address this difficult challenge. In this systematic review, we have summarized recent advancements in biosensor-based detection of these pandemic viruses including COVID-19. Biosensors are emerging as efficient and economical analytical diagnostic instruments for early-stage illness detection. They are highly suitable for applications related to healthcare, wearable electronics, safety, environment, military, and agriculture. We strongly believe that these insights will aid in the study and development of a new generation of adaptable virus biosensors for fellow researchers.**

***Index Terms*— Biosensor, COVID-19, Ebola, Influenza, Pandemic, Rapid detection, Zika**

Manuscript received XXXX, 2021; revised XXXX, 2022; accepted XXXX, 2022. Date of publication XXXX, 2022; date of current version XXXX, 2022. "This work is funded by grant number 12-INF2970-10 from the National Science, Technology and Innovation Plan (MAARIFAH), the King Abdul-Aziz City for Science and Technology (KACST), Kingdom of Saudi Arabia, and in part by funding from the Natural Sciences and Engineering Research Council of Canada (NSERC)."

Shobhit K Patel is with the Department of Computer Engineering, Marwadi University, Rajkot-360003, Gujarat, India (email: shobhitkumar.patel@marwadieducation.edu.in).

Jaymit Surve is with the Department of Electrical Engineering, Marwadi University, Rajkot-360003, Gujarat, India (email: jaymit.surve@marwadieducation.edu.in).

Juveriya Parmar is with the Department of Mechanical and Materials Engineering, University of Nebraska - Lincoln, 1400 R St., Lincoln, Nebraska 68588, USA (juveriyaparmar2@gmail.com). She was with the Department of Electronics and Communication Engineering, Marwadi University, Rajkot-360003, Gujarat, India

Francis M. Bui are with the Department of Electrical and Computer Engineering, University of Saskatchewan, 57 Campus Drive, Saskatoon, SK S79 5A9, Canada. (email: francis.bui@usask.ca)

Kawsar Ahmed is with the Department of Electrical and Computer Engineering, University of Saskatchewan, 57 Campus Drive, Saskatoon, SK S79 5A9, Canada and also working with the Group of BioinformatiX, Department of Information and Communication Technology, Mawlana Bhashani Science and Technology University, Santosh, Tangail-1902, Bangladesh (email: kawsar.ict@mbstu.ac.bd)

Fahad Ahmed Al-Zahrani is with the Dept. of Computer Engineering, Umm Al-Qura University, Mecca 24381, Saudi Arabia. (email: fayzahrani@uqu.edu.sa)

Corresponding Author: K. Ahmed (e-mail: k.ahmed.bd@ieee.org; k.ahmed@usask.ca and kawsar.ict@mbstu.ac.bd)

I. Introduction

THE 21st century has introduced very deadly, dangerous, and infectious diseases to humanity such as influenza virus, Ebola virus, Zika virus, and the most infectious severe acute respiratory syndrome coronavirus (SARS-CoV), and SARS-CoV2. These viruses caused epidemics and pandemics that humankind has never faced before. But the pandemics that we are experiencing in the 21st century have their roots in the mid or late 20th century. These viruses have been around since the 20th century and evolving, and in some scenarios, they have aggravated [1]–[3]. Even though the current epidemics in South Africa are disastrous, the Ebola virus first appeared in the 1970s. In the same manner, the Zika virus was first identified in Uganda in febrile rhesus macaque monkey in the Zika forest and later detected in Aedes Africans mosquitoes in the same forest [4]. In 1954 the first 3 human cases were detected in Nigeria [5] and later it was at large in Brazil from 2015 to 2017 and was reported in 87 countries by late 2019 across the world. Even the latest COVID-19 pandemic has its first appeared in the 1960s and later more than 30 variants emerged as Human coronavirus OC-43 (HCoV-OC43), SARS-CoV, HCoV- NL63, HCoV-HKU1, Middle East Respiratory Syndrome coronavirus (MERS-CoV), and the recent COVID-19 has spread worldwide at large compared to previous coronaviruses [6]–[8].

Reverse transcription polymerase chain reaction (RT-PCR), cell structure, and fast antigen testing are among the major H1N1 medical testing used in hospitals and healthcare facilities. A cotton swab is utilized to collect a sample from the nasopharynx, which is then used for diagnosis in all three techniques [9]. RT-PCR and cell structure are extremely sensitive and precise, unfortunately, they take much time to validate and require costly instruments [10]. The quick antigen assay is affordable and can diagnose a patient in half hour, but it is less robust and precise, and it can't be utilized for validation [11]–[14]. Owing to the low amounts of viremia existing at the beginning of indicators, even screening procedures based on RT-PCR technology might produce false negative results within several days of infectivity [15], [16]. The longer an individual's diagnosis is prolonged, the higher percentage of the

This article has been accepted for publication in IEEE Reviews in Biomedical Engineering. This is the author's version which has not been fully edited and content may change prior to final publication. Citation information: DOI 10.1109/RBME.2022.3212038

virus is present in their body fluids, increasing the chance of infection. The PCR test is the standard method for SARS-CoV-2 identification; nevertheless, it is prohibitively expensive, requires specialized laboratories and expert personnel, and takes longer [17]. Biosensors can be fabricated by employing various techniques that include sputtering, lithography, and the latest printing techniques, and other than these chemical vapor deposition, electrodeposition, electrochemical exfoliation, self-assembly, and electrospinning are some of the well-known fabrication techniques [18]. Furthermore, each fabrication techniques have their advantages and limitations. But among these techniques lithography is widely used for its accuracy but it requires expensive systems for nanoscale fabrication and new masks when featuring design changes. And then there is self-assembly which can provide high resolution with inexpensiveness so we can conclude that self-assembly is an easy fabrication technique [19].

As a result, developing rapid, repeatable, commercial, user-friendly, precise, and early detection of all these pandemic viruses in various specimens is critical. So, it is clear that the rapid, accurate, efficient and low-cost detection of these pandemic viruses will help the medical personnel to start the treatment as early as possible as time is the key factor for saving the patient's life. Tremendous efforts are being made around the world to overcome this constraint by designing suitable, rapid, and consumer-friendly diagnostic tests that can be used at the point of necessity [20]–[22]. The biosensor technique is one of the greatest qualified to address this difficult challenge. Biosensors are comprehensive devices that combine explicit antibodies, enzymes, or DNA strands with an electrochemical, optical, or mechanical transducer in such a means that once the targeted analyte interacts with the bioreceptor, the transducer produces a sequence of physico-chemical variations that can be decoded into comprehensible and assessable signals for numerical analysis. In this context, biosensors play a major role in the detection of these viruses as it has a significant advantage, including a short processing time and excellent selectivity for a variety of biological species. Several biosensor applications are discussed in detail by Patel and co-authors [23], [24].

Different immobilization procedures can create biosensors. Biosensors have boosted interest in immobilization techniques. Biosensors used polyphenol oxidase (PPO). Banana Polyphenol oxidase was purified and immobilized on chitosan-gelatin. Comparing immobilized and free enzyme characteristics [25]. As a result of the evolution of receptors for biological compounds over millions of years, scientists are currently designing hybrid devices using nanoscience and biology, known as Nano-biosensors so that they can detect molecules in extremely small concentrations, inaccessible regions, and even within cells [26]. Small RNAs (miRNAs) have been demonstrated to have regulatory effects on a variety of cellular processes and pathways, including metabolism, viral replication, and cell development [27]. Droplets of varying sizes are the primary means by which the COVID-19 infection spreads. In the beginning, the SARS-CoV2 virus causes a severe respiratory infection that mimics acute respiratory syndrome. Histopathological approaches must be used to identify COVID-19 in samples with a high risk of infection [28]. RSV and HRV cause infants' respiratory epithelium to manufacture inflammatory interleukins (ILs). This study compared RSV-negative and RSV-positive patients' interleukin-8 levels. RSV-positive patients may have higher IL8 levels than RSV-negative ones; IL8 production tends to be released into the nasopharyngeal region, and the evaluation approach can also alter outcomes [29].

In this review paper, we have presented an in-depth and comprehensive survey of pandemic viruses including the latest COVID-19 virus, H1N1 influenza, Ebola virus, and Zika virus detection using the rapid detection technique of biosensing in sections 2 to 5. We have included the recent advances in virus detection that includes thorough data related to the field-effect transistor biosensors, electrochemical biosensors, graphene-based biosensors, nanomaterials-enabled biosensors, label-free biosensors, nanophotonic biosensors, a fiber-optic biosensor, luminescent biosensors, DNA-based biosensors, and some hybrid biosensors that provide a rapid, accurate, sensitive and low-cost diagnosis of pandemic viruses. The concluding remarks are presented in section 6. The insights under this review paper are intended to serve as a foundation for future biosensors' development for all viral diseases.

II. COVID-19 DETECTION

In December 2019, a string of pneumonia cases with no known etiology was recorded in Wuhan, China's Hubei province [30]. Later, the 2019 novel coronavirus (2019-nCov) was discovered in a patient's bronchoalveolar lavage fluid [31]; the International Committee on Taxonomy of Viruses [32] labeled it severe acute respiratory syndrome coronavirus 2 (SARS-CoV- 2) On March 12, 2020, the World Health Organization (WHO) declared the COVID-19 outbreak a pandemic because to the rapid growth in human-to-human transmission [33]. Since the first case was recorded in Nov 2019, the novel-coronavirus COVID-19 has spread to 188 countries and 25 territories all over the globe, regardless of the combined efforts of WHO and governments to control the infection [34]. Since the pandemic started, SARS-CoV-2 has also mutated and formed into several variants as it is the nature of the RNA virus. According to WHO, COVID-19 had been confirmed in over 537 million instances around the world as of June 20, 2022, resulting in 6.32 million deaths [35]. We have seen the many deadly variants of COVID-19 including Alpha, Gamma, Delta, etc. Even if the vaccines are available but still the danger is not over yet. A new variant of COVID-19, named Omicron is found in multiple countries that are more infectious and spreading rapidly all over the world since Nov 2021. All the variants of concern, variants of interest, and variants under monitoring are presented in a table form in Table 1. Mahmud et al. implemented a transcriptomic analysis to identify COVID-19 [36]. Starting from Omicron's appearance, it had spread worldwide; increased hospitalizations; demonstrated greater severity in young people; attacked defense mechanisms of natural immunity; was not resistant to available vaccines. To manage COVID-19 effectively and successfully, available options had to be efficient in the face of

TABLE I
MUTATED STRAINS OF COVID-19 DESIGNATED AS VARIANTS OF INTEREST (VOIS) AND VARIANTS OF CONCERN (VOCS) AND VARIANTS UNDER MONITORING (VUMS) [37]

WHO Label	Pango Lineage	GISAID Clade	Nextstrain Clade	Additional amino acid changes monitored	Earliest documented samples	Date of Designation
Alpha	B.1.1.7	GRY	20I (V1)	+S:484K +S:452R	United Kingdom, Sep 2020	Dec 18, 2020
Beta	B.1.351	GH/ 501Y.V2	20H (V2)	+S:L18F	South Africa, May 2020	Dec 18, 2020
Gamma	P.1	GR/ 501Y.V3	20J (V3)	+S:681H	Brazil, Nov 2020	Jan 11, 2021
Delta	B.1.617.2	G/ 478K.V1	21A, 21I, 21J	+S:417N +S:484K	India, Oct 2021	VOI: Apr 4, 2021 VOC: May 11, 2021
Lambda	C.37	GR/ 452Q.V1	21G	-	Peru, Dec 2020	Jun 14, 2021
Mu	B.1.621	GH	21H	-	Colombia, Jan 2021	Aug 30, 2021
Omicron	B.1.1.529	GRA	21K, 21L, 21M	+R346K	Multiple countries, Nov 2021	VUM: Nov 24, 2021 VOC: Nov 26, 2021

these difficulties [38]. SARS-CoV-2 transmits by respiratory droplets, aerosols, airborne, and particulate matter. Nano-enabled photoelectrochemical oxidation (PECO) assisted air purification is a good technological alternative [39]. Intelligent sensor systems combined with IoTs and AI techniques with 2D nanomaterials have transformed sensor applications in wearable electronics, healthcare, environment, safety, defense, and agriculture [40]–[47]. Due to new SARS-CoV-2 variations, the severity of COVID-19 has worsened, causing health authorities to reevaluate pandemic management techniques. This is crucial due to widespread infection and the global healthcare system's flaws [48], [49]. Low-level detection of a selected disease biomarker (pM level) is valuable for monitoring disease development. Bioinformatics and multi-aspect-oriented analytics are needed to examine treatment effectiveness, optimize therapy, and correlate biomarker levels with illness pathogenesis [50]. Ahmadivand et al. focus on making a tiny plasmonic immunosensor based on toroidal electrodynamics that can sustain ultranarrow plasmonic modes at THz frequencies [51].

Taz and co-authors mainly focused on detecting gene expression profiles for epithelial cells of human lungs caused by SARS-CoV-2 infections and carried out a genomic analysis to confirm the genomic variance between SARS-CoV and SARS-CoV-2 [52]. Zamzami fabricated a carbon nanotube field-effect transistor-based biosensor with high selectivity with SARS-CoV-2 S1 antigen detection in the 10mM Ammonium acetate buffer with a limit of detection of 4.12 fg/mL [53].

A. Electrochemical microbiosensor based detection

Electrochemical-based biosensors are highly utilized given their ease of access, precision, rapidity, a very low limit of detection (LOD), and high sensitivity-like features for the detection of the biomarker regardless of any pretreatment requirement [54]–[56]. Electrochemical biosensors with highly sensitive and selective features were developed by applying the Au, and Ag-based nanomaterials to update the traditional electrode design [57]–[60]. El-said et al. developed the highly sensitive and selective Au micropattern-based highly uniform electrochemical biosensor with increased conductivity for the detection of COVID-19 [61]. The cyclic voltammetry (CV) and square wave voltammetry (SWV) schemes based on COVID-19 monitoring are presented that utilize COVID-19 antibodies as probes. This biosensor detected a wide series of compositions of COVID-19 protein from 5000 pmol/L to 0.1 nmol/L with a LOD of 0.276 pmol/L using the square wave voltammetry method. The real-time usage of this biosensor is validated by obtaining the sample from a human's nasal swab, without any requirement of sample preprocessing.

A dynamic model of the COVID-19 electrochemical biosensor is shown in Fig. 1(a). To obtains the COVID-19 protein, we first integrated the antibody onto a Gold pattern and employed it as a particular probe for S protein. The Atomic Force Microscope (AFM) technique is also used to investigate the topography of this substrate, revealing the production of a uniform gold pattern with a width of about 500 nm and a length of about 1 μm, as shown in Fig. 1(b). Raman spectroscopy is being used to confirm the direct implantation of 50 μM antibody onto the gold pattern.

The efficiency of the proposed SWV-based sensor was also investigated. Fig. 1(c) depicted the square wave voltammetry voltammograms of an antibody/Gold pattern electrode after interrelating with various portions of COVID-19 protein ranging from 5000 fmol/L to 0.1 μmol/L. The value of current is strengthened as the protein concentration rises, according to the research. Fig. 1(d) depicted the link between COVID-19 protein portions and the associated current peak at about 450 mV, which exhibited linear plots with a slope of 3.22 and R^2 of 0.988 within this concentration range. The developed sensor's LOD was found to be 276 fmol L^{-1} using the SWV approach. The real-time detection was also followed by first confirming COVID-19 using PCR validating the presence of the RNA gene of COVID-19 that obtained the oxidation peak at 300 mV and a cathodic peak at 100 mV. To conclude proposed biosensor exhibited high sensitivity toward COVID-19 protein and is capable to detect COVID-19 in human specimens without any complex specimen processes.

B. Nanophotonic biosensor based detection

A point of care (POC) nanophotonic biosensor for the straight, efficient, and precise detection of COVID-19 from both human specimens and animal sources is being developed

This article has been accepted for publication in IEEE Reviews in Biomedical Engineering. This is the author's version which has not been fully edited and content may change prior to final publication. Citation information: DOI 10.1109/RBME.2022.3212038

as part of the European CONVAT project [62]. The technique can be used in isolated surroundings to enhance initial analysis and patient management, besides monitoring the coronavirus environment to avoid future epidemics. CONVAT presents a novel biosensor based on interferometric technology, which has previously been validated for highly sensitive detection of biomarkers and pathogens [63], [64]. The main aim of CONVAT project is to advance a POC biosensor prototype for precise and efficient detection of the SARS-CoV-2 in a short time even in isolated surroundings. The low footprint and great scalability enabled by the fabrication of semiconductors are some of the technology's main advantages. These features make this technology appropriate for multiplexed investigation, where the analytical value enhances as the panel size grows. In addition, unlike many common approaches, which use endpoint-based detection methodologies, real-time surveillance speeds up test progress and allows for direct inspection of biological intellection [65], [66].

A BiMW biosensor's schematic diagram is available in Fig. 1(e). Conventional silicon microelectronics technology is used to manufacture the BiMW sensor chip. Waveguides of micro/nano dimensions are used in the BiMW technology's design. The materials were chosen for their strong refractive index contrast, which is required for a highly sensitive waveguide-based transducer. The BiMW sensor surface is customized with particular receptors targeting exterior antigens of the virus, such as the Spike (S) protein of COVID-19 as shown in Fig. 1(f). The virus traces are acquired by the receptors on the sensor surface once the card is inserted into the biosensor, resulting in an interferometric signal that is logged in real-time. Because the sensor response is proportionate to the composition of viruses in the specimen, the viral load in the patient may be accurately quantified. The bioreceptors must be chosen carefully since they provide both the required affinity and specificity to the assay. While antigen-based tests can be used to screen for and identify COVID-19 contagion, the comparatively minor changes in viral proteins across various virus categories may cause bioreceptor cross-reactivity challenges. The assay is basic, requiring just prior RNA abstraction and disintegration from the virus, which can be implemented quickly after specimen assortment. After the specimen was injected into the device, complementary single-stranded DNA (ssDNA) capture the specific target gene fragments, establishing a duplex chain and resulting in real-time signals proportionate to the number of viruses as shown in Fig. 1(g). The BiMW biosensor's high levels of sensitivity indicate that the unique POC diagnostic equipment will operate efficiently, with LOD in the region of 102–103 viruses per milliliter for straight and fast SARS-CoV-2 virus detection. Given that most COVID-positive patients have viral counts in the span of 105–107 viruses per milliliter, this result is a decent indication that the CONVAT technique may be able to detect even asymptomatic cases with small viral levels. In terms of the genomic assay, the capacity to identify minute amounts of RNA (aM-fM levels) in a straightforward manner in only 30 minutes will considerably improve the accuracy of COVID-19 diagnosis in large inhabitant testing. The device might be used for routine diagnostic analysis of a wide range

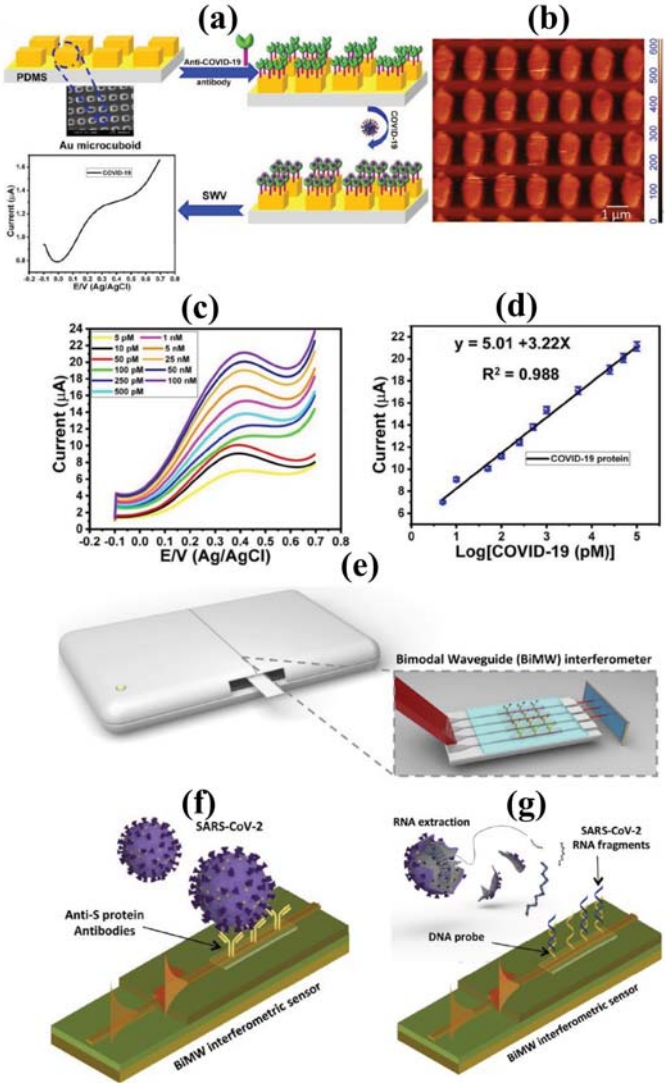

Fig. 1. Various COVID-19 detecting biosensors (a) Illustrative prototype of COVID-19 electrochemical micro-biosensor including immobilization of antibody and obtaining COVID-19 protein (b) AFM topography of the gold assembly (c) SWV voltammograms for different compositions of COVID-19 protein from 5000 fmol L-1 0.1 µmol L-1 after interacting antiCOVID-19 electrode (d) the relation among the composition of COVID-19 protein and oxidation current peak (Reprinted from [61], copyright Springer Nature) (e) A POC biosensor based on biomedical waveguide (BiMW) interferometric technology (f) Detection of intact SARS-CoV-2 using BiMW with CONVAT technique (g) Viral genomic analysis using BiMW with CONVAT technique (Reprinted from [62], copyright IOPSCIENCE)

of diseases and medical conditions, and it could be employed in hospitals, laboratories, and primary care centers. The chips can be mass produced using traditional fabrication techniques, resulting in an affordable system that is projected to be under 15 € per assay.

C. Electrochemical biosensor based detection

COVID-19 diagnostic tests can be divided into two categories: serological and viral nucleic acid assays. The first testing determines the existence of antibodies generated by an individual as a result of virus infection or the presence of antigenic viral proteins in infected patients. Rolling circle

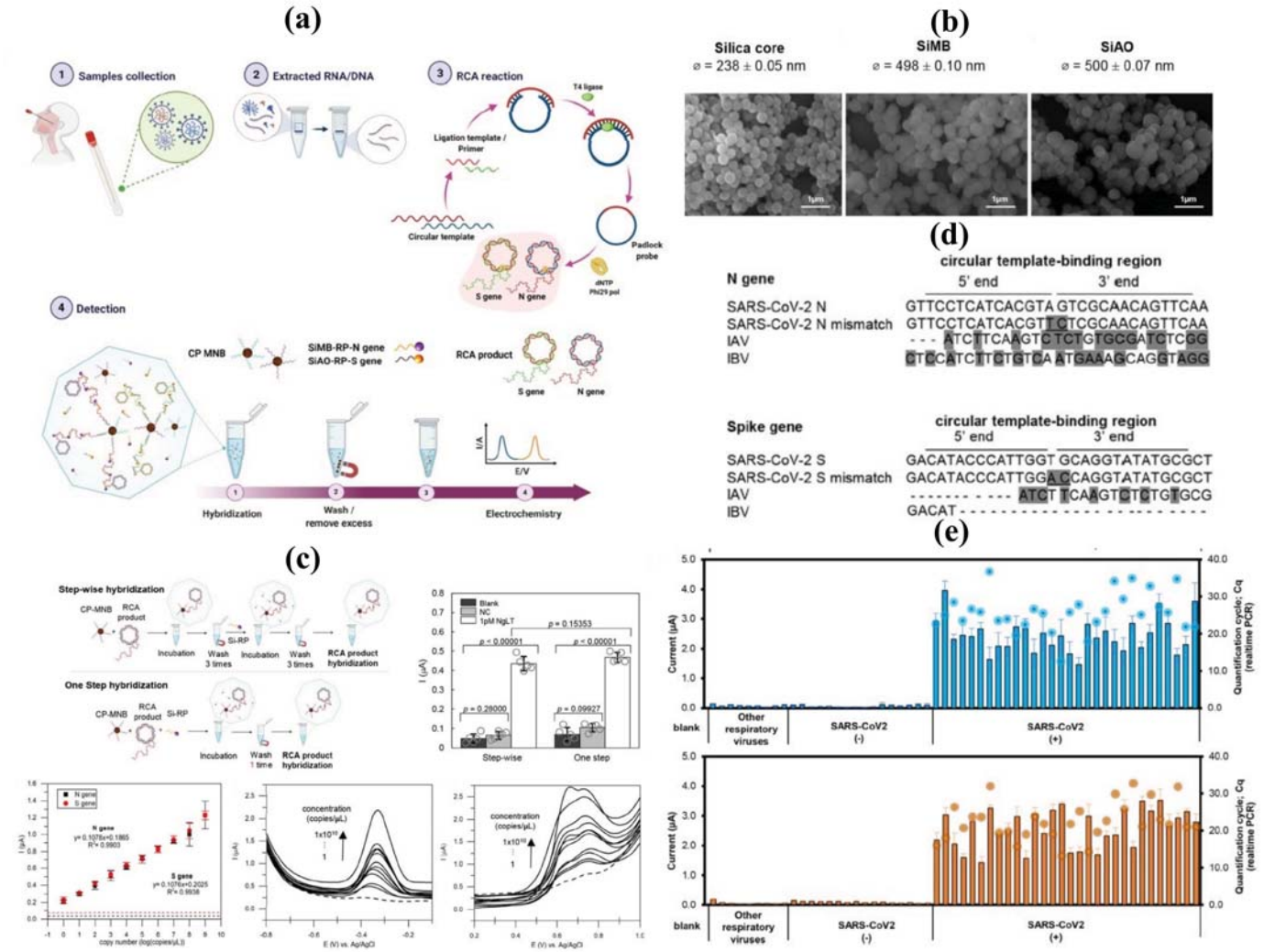

Fig. 2. Electrochemical biosensor-based nucleic acid testing (a) Brief workflow of the biosensor with N genes and S genes RCA, SEM images (b) Silica core, silica-methylene blue (SiMB), and silica-acridine orange (SiAO) with various diameter size represented as mean value with standard deviation (c) Comparison of step-wise and one-step sandwich hybridization process with N gene as the target, No significant difference is observed in these two strategies with sensitivity test for N and S genes positive correlation for a current response, increment in differential pulse voltammetry as N and S gene concentration increases (d) Numerous sequence position of N genes and S genes target orders with mismatch and non-complementary target orders. Dark areas and underlined bases show the non-complementary arrangements to the target gene and mismatch bases, respectively (e) The identification of N genes and S genes in 55 cDNA specimens equated with the Cq result from qRT-PCR (N genes (Blue dots), S genes (Orange dots)) (Reprinted from [69], copyright Springer Nature)

amplification (RCA), an isothermal amplification method, has also been frequently utilized for nucleic acid testing [67]. With little reagents, RCA can yield amplicons 109-fold in 90 minutes [68]. Chaibun et al. reported an electrochemical biosensor for the rapid detection of the S gene and N gene of SARS-CoV-2 from the clinical specimen as shown in Fig. 2(a) [69].

In less than 2 hours, the test could identify as few as 1 copy L-1 of viral N or S genes. Clinical specimens were utilized to assess the test's efficiency, which is shown to be consistent with the results of qRT-PCR. Through surface-reactive functional groups, two redox dyes, MB and AO, were coated onto silicon nanoparticles. SEM images of SiMB, and SiAO are shown in Fig. 2 (b). In comparison to the silica core, the size of the silicon nanoparticles after coating with the redox dye increased. The current signal for the two techniques did not differ significantly as the p-value is less than 0.05 (Fig. 2c). As a result, the single-step hybridization approach was applied for the enhanced test because it was comparatively easy, rapid, and required fewer preprocessing steps. The rise in electrochemical signals was certainly linked with the rise in gene copy amount for the S genes and N genes as well (Fig. 2c).

The respiratory infections COVID-19 and influenza are both infectious. COVID-19 and influenza have nearly identical symptoms, despite the fact that they are caused by separate viruses. It might be difficult to tell the difference only based on medical symptoms. To avoid misclassification, an analytic assay that could identify the influenza virus from SARS-CoV-2 is essential. 1 pM of non-complementary target orders of Influenza A and Influenza B viruses was used in the specificity testing, with the sequence alignment displayed in

This article has been accepted for publication in IEEE Reviews in Biomedical Engineering. This is the author's version which has not been fully edited and content may change prior to final publication. Citation information: DOI 10.1109/RBME.2022.3212038

Fig. 2(d). There was additionally 1 pM of linear targets with two bases mismatch added which is also presented in Fig. 2(d). A positive result was defined as a current signal that was equivalent to or more than +3 standard deviations above the average mean of the background signal. In RCA, RNA and cDNA specimens produced from clinical specimens were employed as the template, with electrochemical detection and one-step hybridization. As shown in Fig. 2(e), including 30 cDNA and 11 RNA totaling 41 specimens prepared from COVID-19 +Ve specimen produced +Ve results, whereas the including 25 cDNA, 40 RNA totaling 65 specimens prepared from COVID-19 -Ve specimen produced -Ve results. This matched the results of the qRT-PCR. The limit of detection (LoD) of the proposed assay demonstrated that it is incredibly sensitive compared to already accessible assay kits and prevailing biosensors.

D. Protein-based biosensor for detection

Biosensors for cellular and clinical applications have been developed using naturally occurring protein switches [70]. Authors anticipated that these properties may be achieved by the presence of a peptide actuator controls They implemented a model that consists of two protein elements: a 'lucCage,' which consists of a cage domain and a latch domain containing a target-binding motif and a split luciferase fragment; and a 'lucKey,' which consists of a key peptide that ties to the open state of lucCage as shown in Fig. 3(a). As illustrated in Fig. 3(a) right side, when lucKey and lucCage are combined, luciferase activity is reconstituted. In the absence of a target, the binding energy of Luckey to lucCage is not enough to surpass the free energy charge of lucCage opening, for the tuning of thermodynamics of the system, as shown in Fig. 3(b). The author's incorporated sensors that can directly detect COVID-19 viral particles, as shown in Fig. 3(d). As available in Fig. 3(c), each sensor responds quickly. Table 2 presents the comparison study of available COVID-19 detecting biosensors based on their limit of detection (LOD) and other important details.

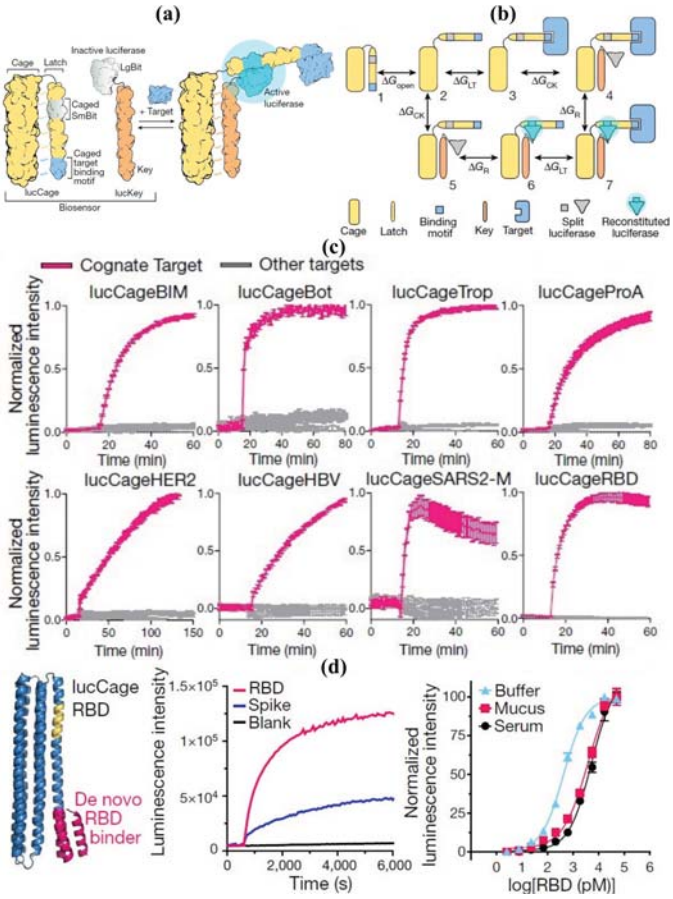

Fig. 3. (a) Illustrative mechanism of the proposed sensor (b) The thermodynamics behind the activation of sensor (c) Specificity of the proposed sensor for various cognate targets and targets for other biosensors (d) Incorporating of de novo SARS-CoV-2 RBD binder, Increment in luminescence due to the addition of trimeric spike protein, and detection over a range of analyte compositions in buffer (Reprinted from [71], copyright Springer Nature)

III. INFLUENZA DETECTION

The influenza virus, often called flu, is an extremely severe respiratory illness, including the 1918 Spanish influenza H1N1, 1957 H2N2, 1968 H3N3, and the 2009 H1N1 influenza has impacted millions of individuals around the globe, and innumerable financial and social costs [89]–[91]. Conferring to the WHO, 2000 million individuals are diseased with flu-like pathogens comprising Influenza, among these $250k - $500k worldwide annual deaths are reported [92]. After that new animal-originated influenza viruses such as H5N1, H7N9, and H9N2 have infected humans on rare occasions but had not been transmitted at large [93], [94]. However, extended mutation of these viruses could steer to full adaption to humans and high and long-term transmission capabilities. Since its first apparition in 2013, the influenza H7N9 virus has spread the most, with 1,567 laboratory +Ve human infectivity [95]. Since the establishment of the benchmark in virological diagnostics – viral separation from tissue structures or embryonated chicken eggs – multiple approaches for rapid (< 2 h) detection of the influenza virus have been established. The majority of modern approaches rely on PCR (conventional PCR, RT-PCR, etc.) [96]–[99] or immunoassay technologies [100]. PCR technologies have more sensitivity and specificity than other molecular procedures, and they take less time [101].

A. Boron-doped Diamond-based biosensor for detection

Nidzworski and co-authors presented a biosensor for the early detection of the influenza virus [102]. The findings allow for high-precision, high-throughput influenza virus detection of the virus. The reason behind choosing the M1 (matrix) protein as a detection target is that it is the sole viral element required for the generation of VLPs (virus-like particles) and is found in very influenza virus serotypes.

For the precise detection of the influenza virus, a label-free, highly sensitive biosensor was developed and evaluated. High sensing capability and great stability are features of the improved BDD electrodes. Furthermore, the findings show that the proposed method has a number of advantages over existing methods, including a short detection and incubation time (less

TABLE II
COMPARISON TABLE OF COVID-19 DETECTING SENSORS WITH PREVIOUSLY PUBLISHED WORK

Sensor Design	**Sample**	**Target**	**Limit of Detection (LoD)**
Ref [72]	-	S protein	5 nmol/L
Ref [73]	Oropharyngeal swabs	N gene	0.18 ng/μL
Ref [74]	Synthetic RNA	Conserved region	0.96 pmol/L
Ref [75]	SARS-CoV-2 antigen protein and MERS-CoV protein; nasopharyngeal swabs	Spike protein antibody	100 fg/mL
Ref [76]	COVID-19 spike antigen in saliva	S protein	10 fM
Ref [77]	RNA (RdRp)	-	0.5 ng
Ref [78]	ORF1ab and N genes	-	12 copies/reaction
Ref [79]	SARS-CoV-2 RNA	-	10 copies
Ref [80]	-	-	3.5 ng/mL
Ref [81]	Nasal swab	ORF1ab and N gene	2 copies/sample
Ref [82]	Nasopharyngeal swabs	E gene and N gene	10 copies/ μL
Ref [83]	-	S, N, and ORF1ab genes	42 copies/reaction
Ref [84]	Synthetic cDNA	RdRp	2.26 $\times 10^4$ copies
Ref [85]	Swabs and bronchoalveolar lavage fluid	ORF1ab	20 copies/reaction
Ref [86]	Throat swabs	S gene	200 copies/reaction
Ref [87]	Nasal swabs	N gene	100 copies
Ref [88]	Synthetic cDNA	RdRp	0.4 fM

than 5 minutes), extremely high sensitivity (LOD 1 fg/ml), stability, and high repeatability in influenza virus detection, and the ability to perform consistently. In comparison to currently utilized analytical procedures, this technique has the shortest investigation time and the lowest LOD. The difference in charge transference resistance was even small than 10% and was consistent across all verified electrodes. Given the extensive application of this strategy, the authors are confident that the current findings will result in significant improvements in medical analytical approaches in the near future.

B. DNA 4WJ based Electrochemical biosensor for detection

Park et al.presented a biosensor comprised of 4-way junction (4WJ) and carboxyl-MoS2 hybrid material to accurately detect H1N1 [103]. The hemagglutinin aptamer was placed on the recognition part (head group), four silver ions were placed on each of the two arms (signal amplification part), and an amine group was placed on the tail group (anchor). This manufactured multifunctional DNA four-way junction can bind to hemagglutinin specifically and selectively. Furthermore, the carboxyl-MoS2 improves the sensitivity of this biosensor. An electrochemical study revealed the existence of H1N1 when it was inserted into the immobilized electrode. It was also able to establish whether this sensor responds explicitly and selectively to the influenza virus (H1N1) through selectivity testing. It is also confirmed that the biosensor responded linearly to influenza and that influenza could be sensed at concentrations ranging from 0.1 μM to 0.01 nM. Finally, laboratory experiments using human serum diluted hemagglutinin exhibited an analogous inclination to those using water diluted hemagglutinin. The multi-functional DNA four way junction and carboxyl-MoS2 hybrid substance can be used to make an electrochemical influenza virus (H1N1) detecting biosensor, according to this study.

The multifunctional DNA 4WJ has comprised of four ss-DNA molecules that each have a significant characteristic. In the head and tail sections of this 4WJ, the influenza aptamer and amine group were inserted. The DNA aptamer attaches to a specific target molecule. Easy adaptation to the needed form, minimal rate of manufacturing via chemical combination, great stability, and minimal cost production are only a few of the benefits. An addition of carboxyl-MoS2 enhanced the sensor's sensitivity. Field-emission SEM was utilized to confirm the synthesis of carboxyl-MoS2, and AFM was used to confirm the immobilization process of each stage. Furthermore, the detection was found to be possible at concentrations ranging from 0.1 μM to 0.01 nM. The LOD of 0.01 nM was achieved. It was also established that this sensor exclusively reacted to H1N1 by conducting the selectivity test. Furthermore, studies revealed that the proposed bioprobe can be employed in real-world scenarios.

C. Label-free biosensor for detection

Many researchers have concentrated on analyzing the impacts of linking architectures of sialic acid clusters in host receptor compound glycans, which differ from class to class because HA receptor explicity is a major aspect in the progression of contagion, spread, and adaptability of influenza viruses [105]. The N-acetylneuraminic acid, 2,6, galactose (α2,6 associated sialic acid moieties), is presented in Fig. 4(a), which are predominantly located on the epithelial units of the human upper ventilatory tract, exhibit a binding preference for human adapted influenza HA proteins [106]. Animal influenza HA proteins, on the other hand, target the NeuAco2,3Gal (2,3 linked sialic acid moieties), which are prevalent in epithelial units of the entrails as well as the entire ventilatory system of animals and birds [107]. Numerous researchers have shown that the alteration in the linking architectures of 2,6 vs 2,3 sialic acids impacts the capacity of influenza viruses to affect various classes, despite its apparent insignificance [108]. Although PCR is the prime standard for detecting the H1N1 virus, it cannot identify the ventilatory-binding explicity of remote influenza (H1N1) virus a priori. As a result, sensors for quickly determining HA ventilatory explicity, particularly the distinction of influenza HA proteins binding 2,6 and 2,3 associated sialic acids, are crucial for evaluating the adaptative capabilities of newly developing animal influenza viruses.

Label-free sensor systems capable of profiling influenza HA glycan binding explicity in a microarray style are therefore extremely required. To meet this prerequisite, Zhang et al. used the Arrayed Imaging Reflectometry (AIR) sensor platform to produce and evaluate microarrays of influenza ventilatory-binding analogues [104]. AIR is a multiplex detection system that does not require the use of labels. The platform makes use of a single-camera interferometric imaging setup. A charge-coupled device (CCD) camera captures the array's reflected

This article has been accepted for publication in IEEE Reviews in Biomedical Engineering. This is the author's version which has not been fully edited and content may change prior to final publication. Citation information: DOI 10.1109/RBME.2022.3212038

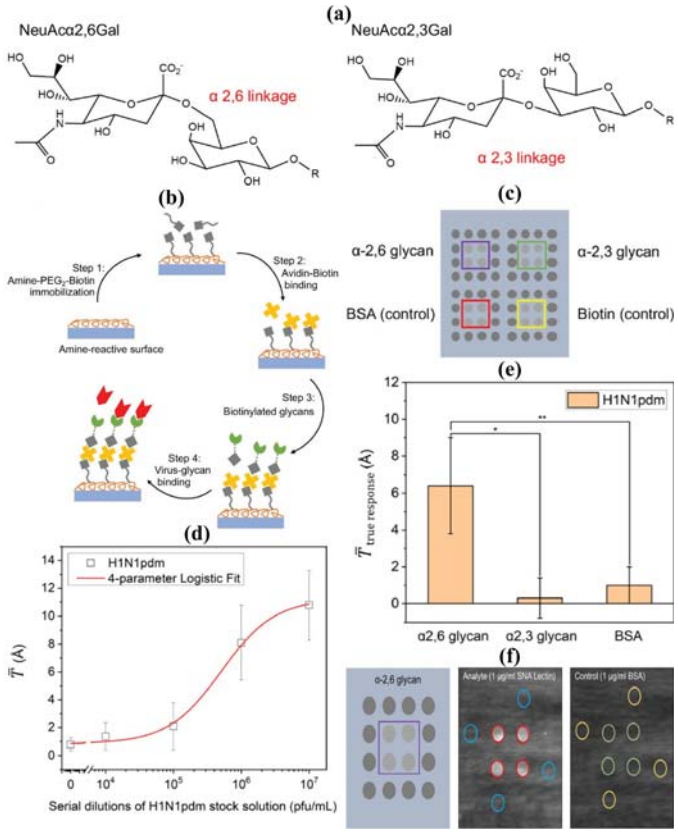

Fig. 4. Label-free, Multiplex microarray biosensor for influenza detection (a) Human and avian cell surface sialyloligosaccharide structures (b) Preparation and incubation of AIR microarray chips for virus-glycan binding detection (c) Glycan-based receptor analogue microarray layout design (d) AIR glycosyl microarray responses to H1N1pdm and H13N8 viruses at various viral doses (e) The glycan microarray's quantitative response data to the H1N1pdm virus (left) and the H13N8 virus at right. (f) Analysis protocol for AIR images (Reprinted from [104], copyright ACS Publications)

image. Figure 4(b) depicts the microarray chip processing and polymer-based glycan-antigen identification method. The microarray layout is shown in Fig. 4(c). As hypothesized, influenza H1N1pdm coupled to the α2,6 linked sialic acid moieties probe sites with remarkable selectivity. Similarly, the H13N8 virus bonded only to the NeuAc2,3Gal linked glycan probe sites, demonstrating that it is species specific. For human and bird influenza viruses, quantified response data approves explicit binding of the virus to individual glycan probe as shown in Fig. 4(e). As illustrated in Fig. 4(d), the AIR microarray pictures were collected, recorded, and examined for quantitative responses. The response values for each array location were determined using an empirically resultant response model to convert the reflection intensity unit to thickness. The response model depicts the connection among reflected intensities measured by ellipsometry and their corresponding thicknesses for various exposures. Figure 4(f) shows an example of this technique employing a chip containing the α2,6 glycan analogue and treated with SNA lectin. Table 3 presents the comparison study of available Influenza virus detecting biosensors based on their limit of detection (LOD) and range of functionality.

TABLE III
COMPARISON TABLE OF INFLUENZA VIRUS DETECTING SENSORS WITH PREVIOUSLY PUBLISHED WORK

Sensor Design	Range	Limit of Detection (LoD)
Ref [109]	5 $\sim$ 50 ng/mL	13.9 pg/mL
Ref [110]	10 $\sim$ 100 nM	3.45 nM
Ref [111]	10 $\sim$ 10000 PFU/mL	3.7 PFU/mL
Ref [112]	200 pg/mL $\sim$	138 pg/mL
Ref [113]	10 pg/mL $\sim$ 10 μg/mL	10.79 pg/mL
Ref [114]	1 $\sim$ 10000 PFU/mL	0.5 PFU/mL
Ref [103]	10 pM $\sim$ 100 nM	10 pM
Ref [115]	0.02 to 3 HAU	29.6 ng/mL
Ref [116]	10^3 to 10^7 pfu/mL	10 μg/mL
Ref [117]	10^3 to $10^7 EID_{50}$/mL	$10^3 EID_{50}$/mL
Ref [118]	10^2 to $10^5 EID_{50}$/mL	$10^3 EID_{50}$/mL
Ref [119]	0.128 $\sim$ 12.8 HAU	0.128 HAU

IV. Ebola Detection

The Ebola virus disease (EVD) epidemic of 2014-15 in West African countries and infrequent cases in Europe and North America has caused thousands of deaths that resulted in worldwide chaos [120]. The Ebola virus is a type A select agent filovirus that was initially discovered in 1976 in Zaire and named after the Ebola River [121]. Person-to-person transmission of Ebola is reflected by direct contact with infected patients, bodily fluids, or compromised clothing. Enhanced disease control actions and primary medication at specialist institutions might be possible if this highly contagious virus could be detected early. The present fatality rate from epidemic Ebola varies from 40% to 90%, and early, point-of-care diagnoses could substantially reduce this number [122], [123]. According to mathematical calculations, the total direct costs of this outbreak in the three most affected nations vary from $82 million to 356 million; early identification and medication will also minimize overall healthcare expenditures [124].

Various ELISA testing, RT-PCR testing, virus separation, electron microscopy, and serologic testing for IgM or IgG antibodies are being employed to identify Ebola. Quantitative viral load testing is also prognostic, with patients with viral loads of more than 10 million copies/mL having a substantially higher case fatality rate [125]. Due to the very small amounts of viremia that exist at the outset of indications, even analytic procedures based on the RT-PCR method might provide false negative outcomes in the first few days of infectivity [126]. The longer a patient's diagnosis is delayed, the more virus is existing in their body liquids, increasing the chance of infection. EVD can also have a long incubation period, up to three weeks, necessitating the use of diagnostic tests. Several diagnostic approaches have been investigated for quick diagnosis of EVD.

A. Surface Acoustic Wave (SAW) biosensor for detection

Rapid Ebola virus diagnosis at the point of care could allow for early containment and the averting of future outbreaks and pandemics [127]. Although there are POC nucleotide intensification tests, they are inadequate by the necessity for several reagents, preservation, and expert persons. Baca and

co-authors presented initial outcomes of a SAW biosensor that has the ability to detect the EVD within 5–10 minutes [128]. SAW sensors can identify EVD antigens fast at the POC, with no additional chemicals, sample processing, or trained people required. The authors utilized a deactivated virus to proceed with this work under non-BSL-4 settings because the fully intact Ebola virus is very infectious.

Prior to virus inactivation, EVD antigens were found in phosphate-buffered saline (PBS) solutions at concentrations ranging from 1×10^4 PFU/mL to 3×10^6 PFU/mL. On the first day of illness symptoms, Ebola patients had an average viremia level of 30 RNA kcopies/mL [129]. EVD detection occasioned in a composition-dependent rise with phase shit values roughly spaning from 16 kPFU mL^{-1} to 6.5 MPFU mL^{-1}. By employing linear regression and the other factors, an Ebola virus limit of detection of 19 kPFU/mL was achieved. These findings show that the prototype SAW biosensor identifies EVD antigens in a specified buffer fast, with LOD under the mean viremia level at the beginning of medical indications.

B. Electrochemical DNA biosensor for detection

Many clinical and environmental investigations have focused on ssDNA identification, such as cancer diagnosis [130], bacterium detection [131], SPR [132], and spectroscopic methods approaches [133]. Electrochemical DNA biosensors stand out because of their distinct advantages, which include affordable, quick reaction, user-friendly, correct selectivity, and high sensitivity.

Ilkhani et al. developed a new electrochemical DNA biosensor for detecting the Ebola virus [134]. The electrochemical biosensor was created by applying S-Au boundaries. The hybridization process was detected using EIS and DPV. Scrutinized using the electrochemical impedance spectroscopy approach and used as a signal for label-free DNA hybridization exposure. The results showed that the EVD DNA can be identified with great repeatability, sensitivity, and selectivity using an electrochemical biosensor. As an analytical technique, this system can be used to detect Ebola virus DNA in genuine samples. This approach can also be used to analyze bacterial pollution in the environment, such as in water or food sources.

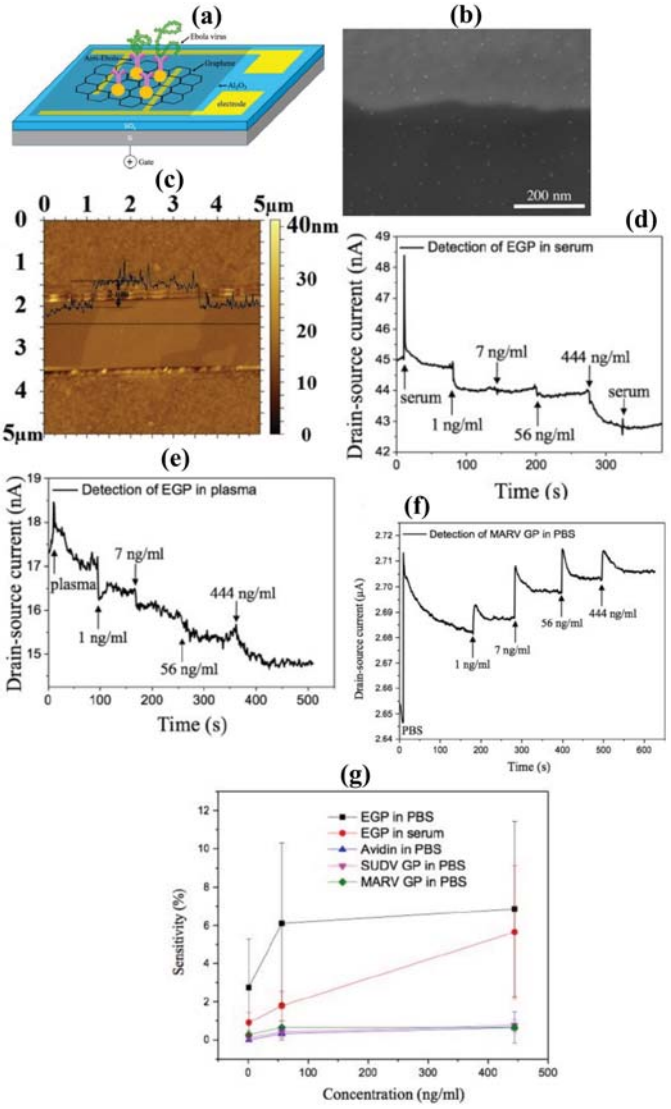

Fig. 5. (a) Illustrative diagram of reduced graphene oxide-based FET biosensor (b) SEM image of reduced Graphene Oxide sheet (c) AFM used to determine the depth of the reduced Graphene Oxide sheet, which was found to be less than 2 nm (d) EGP inserted in $\mathbf{10^{-3}}$ × human serum (e) EGP inserted in $\mathbf{10^{-3}}$ × human plasma (f) Detection of MARV GP in PBS (g) Sensitivity as a function of protein composition is investigated. (Reprinted from [135], copyright Springer Nature)

C. Field-Effect Transistor (FET) biosensor for detection

For real-time detection of the EVD antigen, Chen et al. developed a rGO FET technique [135]. This technology takes advantage of graphene's appealing semiconductor properties to produce a very sensitive and explicit identification of EVD glycoprotein in real time. These findings show that an enhanced FET biosensor for EVD diagnostics may be successfully fabricated. The FET is a potential approach for detecting a variety of analytes quickly and accurately. Its applicability has been established in the detection of target analytes in gases [136] and water [137], for example. Rapid reaction, minimal cost, and ease of use are all advantages of FET sensors. By affixing explicit probes on the conducting channel, FET biosensors can attain improved selectivity and sensitivity, defined as a fundamental feature for FET sensor accomplishment. When compared to graphene prepared by the CVD approach, rGO FET devices may be simply made by thermal annealing graphene oxide sheets, with the added benefits of affordable and empirical pliability. Anti-Ebola probes have been mounted on the channel, and they preferentially catch the antigen. The authors discovered that such a FET biosensor exhibits great fundamental characteristics for the Zaire strain's Ebola GP, with a detection limit of 1 ng/ml.

The Ebola antibody is mounted to identify the particular antigen in Fig. 5(a), which depicts an illustrative structure of the reduced Graphene Oxide-based biosensor mechanism. The design of the produced biosensor device was investigated using SEM as shown in Fig. 5(b). Sputter coating was used to deposit GNPs homogeneously on the mechanism for antibody conjugation. The gold NPs weren't visible prior to sputter

This article has been accepted for publication in IEEE Reviews in Biomedical Engineering. This is the author's version which has not been fully edited and content may change prior to final publication. Citation information: DOI 10.1109/RBME.2022.3212038

TABLE IV
COMPARISON TABLE OF EBOLA VIRUS DETECTING SENSORS WITH PREVIOUSLY PUBLISHED WORK

Biosensor Design	Technique	Target	Dispersion Medium	Limit of Detection (LoD)	Processing Time
Re $EBOV^{TM}$	Chromato- graphy	VP40	Blood, Plasma	625 ng/mL	15-25 min
Ref [135]	FET	EGP	PBS, Serum, Plasma	1 ng/mL	Few seconds
Ref [138]	Chromato- graphy	EGP	Serum	100 ng/mL	30 min
Ref [139]	Chromato- graphy	EGP	Serum	150 ng/mL	-
Ref [140]	Single particle interferometric reflectance imaging sensor	Pseudotyped Ebola Virus	Blood, Serum	5 $\times 10^3$ pfu/mL	2 h
Ref [141]	Opto-fluidic nanoplasmonic	Pseudotyped Ebola Virus	PBS	106 pfu/mL	90 min
Ref [142]	Opto-fluidic chip	Ebola RNA	Water	0.2 pfu/mL	3-10 min

coating, implying that these glowing "dots" are GNPs created by the sputter coater. The depth of the reduced Graphene Oxide sheet is calculated using AFM to better characterize the FET device. The reduced Graphene Oxide sheet has a depth of roughly 2 nm, demonstrating a few-layer structure, while the monolayer depth is 340 μm, as seen in Fig. 5(c). The authors utilized 10^{-3} $\times$ human serum per plasma acquired from the Blood Center of Wisconsin to suspend Ebola glycoprotein as a technique to replicate blood specimen from EVD +Ve persons to examine sensor performance under a more difficult yet real-time environment. The sensor's dynamic response to EGP in 10^{-3} $\times$ serum is shown in Fig. 5(d). As the concentration of EGP increased, the Id decreased as well. The biosensor was then refilled with 0.01 $\times$ serum, but no substantial variation occurred, demonstrating that only explicit binding can cause a current variation. Fig. 5(e) shows the dynamic response to EGP in 0.01 $\times$ plasma, with respect to a significantly noisier signal. The serum/plasma reaction to EGP was similar to that in PBS, but with a decreased sensitivity (about 1.7% for 1 μg L^{-1} Ebola glycoprotein in $10^{-3}\times$ serum), demonstrating the complex dispersion medium affects the response. Fig. 5(f) depicts the dynamic responses to non-specific GP. The sensitivity of 1 ng/ml of MARV GP is just about 0.18 percent. As a result, the FET biosensor has a low reaction to non-explicit glycan proteins and significantly lower sensitivity than the EGP, implying that cross reactivity is low and the sensor has good selectivity for the target protein. In Fig. 5(g), five independent replicates are used to compare the sensitivity of EGP, avidin, SUDV GP, and MARV GP as a function of composition with error bars. Table 4 presents the comparison study of available Ebola virus detecting biosensors based on their limit of detection (LOD), techniques used for detection, processing time, and other important details.

V. ZIKA DETECTION

The first substantial outbreak of Zika fever occurred on the Federated States of Micronesia's Western Pacific Island of Yap in 2007 [143]. Multiple incidences of ZIKV have been recorded since then all across the world. In French Polynesia, two major crises impacting over 30,000 residents occurred in 2013 and 2014 [144], [145]. Smaller epidemics were also reported in New Caledonia, Easter Island, and the Cook Islands, as well as the Solomon Islands, Samoa, and Vanuatu. Later, it was reported in continental South America in Brazil in May 2015 and WHO declared it as a public health emergency in February 2016 as 1.3 million people were infected in Brazil itself. Furthermore, more than 20 countries in the Americas have reported the autochthonous Zika virus transmission, comprising Puerto Rico and US Virgin Islands during 2016 [146].

The US Food and Drug Administration has approved 14 rRT-PCR screening assays and 5 anti-ZIKV IgM serological tests. For a point of care testing (POCT), only one rRT-PCR and four serological screening assays are utilized, with a sensitivity and specificity of more than 90%. These assessments, however, take roughly 1–3 hours to complete [147]. Cross-reaction of ZIKV antibodies particularly with DENV, is possible, thereby increasing false positives in several immunoassays [148]. Furthermore, serological and molecular assays necessitate costly instruments and skills to operate. The majority of ZIKV infections occur in developing nations, which lack adequate laboratory facilities, skilled personnel, and financial resources. As a result, fresh approaches are needed to develop a ZIKV-specific POC scheme that can distinguish between ZIKV and DENV infections in epidemic areas that are efficient, low-cost, and quick.

A. Peptide aptamer pair-linked based biosensor for detection

To identify ZIKV, Nguyen et al. created a new biosensor [149]. A peptide aptamers pair (PAP) were used to create an antibody-free lateral FICT. The LOD for the B2.33-P6.1 PAP for ZIKV in the quick diagnostic strip was 20000 tissue culture infective dose $TCID_{50}$/mL. Significantly, FICT was able to distinguish ZIKV from DENV. Human sera and urine were used to confirm the stability and performance of FICT, and the LOD value was found to be equivalent. In silico modeling was employed to design a novel PAP FICT assay for identifying ZIKV, according to the study.

The TL/CL value was used to calculate the LOD of FICT. At 8 × 10^4 $TCID_{50}$/mL, P29.1 and $Z_{10.8}$, strongly distinguished ZIKV. ZIKV was detected at a higher titer, 320000 $TCID_{50}$/mL, by the -Ve $Z_{10.2}$ peptide in combination with B2.33, which was substantially dissimilar from the +Ve peptides. With satisfactory linear regression, the ZIKV titer related to the limit of detection was 40000 $TCID_{50}$/mL, while the limit of detection was 20000 $TCID_{50}$ mL^{-1}. P6.1 had a considerably greater signal for ZIKV identification with p value less than 0.001, demonstrating that the novel P6.1 peptide detects ZIKV better than the earlier $Z_{10.8}$ peptide, which is a constant with predictions. Peptide aptamers have

been successfully produced by Authors as a useful diagnostic material for distinguishing between ZIKV and DENV. This innovative PAP FICT test could well be conducted in 20 minutes and used as a POC scheme to detect ZIKV in human serum and urine.

B. Gold nanoparticles based electrochemical biosensor for detection

A durable nanobioconjugate relied upon gold nanoparticles (GNPs) connected to ssDNA has been developed for high-sensitivity magnification of the electrochemical signal of a ZIKV [150]. The genosensor is designed with Ru3+ as an electrochemical reporter on a screen-printed gold electrode (SPGE)/screen-printed carbon electrode (SPCE) designed with layered gold nanostructures (SPCE/G). The genosensor performance was straight from 0.01 to 0.6 aM and from 0.5 aM to 0.01 fM of the targets, as measured by DPV, with a sensitivity of 2700 and 2900 mA cm^2 M^{-1} and a LOD of 0.2 and 33 fM at the SPGE and SPCE/G, accordingly. Nanobioconjugates are hybrid nanomaterials formed when nanomaterials and biomolecules are combined [151]. Hundreds of active biomolecules and tags have been immobilized on top of nanomaterials to boost signal strengthening responsiveness. The conjugation of GNPs with ssDNA provides a simple way to synthesize nanobioconjugates with exceptional capabilities for signal amplification, improved sensitivity, and lower LOD in bioassays. A solution in the existence of sodium chloride is shown in Fig. 6(d) and the inset at various enlargements. The DPV plots for highly sensitive identification of the Zika synthetic genetic substance formed at the exterior of SPGEs are shown in Fig. 6(e). With a sensitivity of 2900 nA cm^2 M^{-1} and a LOD of 0.2 fM as illustrated in Fig. 6(f), they exhibit a linear dependency of the electrochemical response with the increasing target composition in the range of 0.01 to 0.6 aM. Serum samples from diseased individuals showed variable current density responses. In comparison to the -Ve control (NC1) with no target, serum specimens from diseased patients demonstrated variable current density outcomes, which might be connected to the RNA loading in every specimen (Fig. 6(g)).

As depicted in Fig. 6(h), the electrochemical sensor was also evaluated in urine and saliva samples doped with 1000 fM synthetic explicit DNA. The research indicated that the signal strength in the urine sample was greater than that in the saliva specimen, even when the target concentration was the same. Table 5 presents the comparison study of available Zika virus detecting biosensors based on their limit of detection (LOD), techniques used for detection, processing time, and other important details.

This is the first GNP-ssDNA nanobioconjugate to be employed in the ultrasensitive recognition of ZIKV genetic substance without the use of specimen abstraction or PCR. The gene-based assay was developed with a Ru3+ complex as an electrochemical reporter on either a SPGE or a SPCE modified with Au layered nanostructures (SPCE/G) as shown in Fig. 6(a). The resulting sensor identified ZIKV genetic substance in raw serum specimens from diseased individuals, confirming the

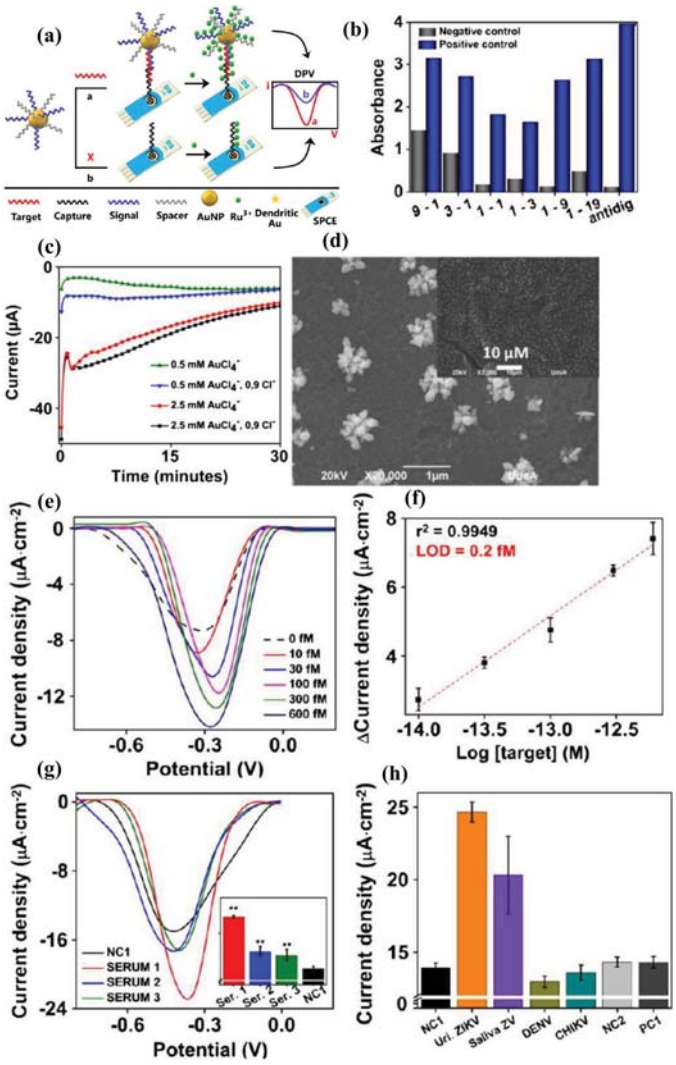

Fig. 6. Gold nanoparticles based electrochemical biosensor based Zika virus detection (a) Illustration of the concept to amplify the nanobioconjugate-based signal (b) Assessment of molar ration using anti-Dig-HRP as a reporter (c) For various gold and NaCl composition, chronoamperometry curves for the gold electrodeposition (d) SEM images of gold resultant structures at various enlargement (e) DPV plots of nanobioconjugates accumulated onto SPGEs and (f) Resultant calibration curve (g) DPV plots of three positive ra serum specimens (h) Matrix effect and specificity (Reprinted from [150], copyright Springer Nature)

nanobioconjugate's ability to amplify signals in a gene-based assay style as well as its huge potential for detecting genetic material at clinically relevant amounts. Fig. 6(b) demonstrates that decreasing the spacer probe composition with maintaining the signal probe one constant reduced the colorimetric and background signal significantly. The colorimetric response increased when the spacer probe composition remained intact while the signal probe composition rose. As a result, the 1:9 ratio of spacers to signal probes is chosen as the ideal proportion for producing stable nanobioconjugates with the best SNR. The chronoamperometry curves and the influence of NaCl on the gold nanostructures electrodeposition are shown in Fig. 6(c). The estimated electric charge values in 500 μM and 2500 μM gold solutions with and without 900 mM NaCl were 1580, 2820, 1820, and 18400 μC, respectively (Fig. 6(c)). The

TABLE V
COMPARISON TABLE OF ZIKA VIRUS DETECTING SENSORS WITH PREVIOUSLY PUBLISHED WORK

Sensor Design	Technique	Target	Range	Limit of Detection (LoD)
Ref [150]	DPV	DNA ZIKV	10 – 600 fM	0.2 fM
Ref [152]	EIS	DNA ZIKV	54 – 340 nM	25 nM
Ref [153]	DPV	DNA ZIKV	1.7 – 1.7 × 10^{10} copies/mL	1.72 copies/mL
Ref [154]	SPR	DNA ZIKV	10 – 10^{7} copies/mL	8.2 copies/mL
Ref [155]	EIS	DNA ZIKV	1 pM – 1 μM	0.8 pM
Ref [156]	Chronoamperometry	DNA ZIKV	5 – 300 pM	0.3 pM
Ref [157]	EIS	NS1 protein ZIKV	10 pM – 1 nM	10 pM
Ref [158]	CV	ZIKV-NS1 antigen	0.1 – 100 ng/mL	1 pg/mL
Ref [159]	SPR	ZIKV-NS1 antigen	10 – 10^{5} ng/mL	1 ng/mL
Ref [160]	Sandwich ELISA	ssDNA aptamer	-	100 ng/mL
Ref [161]	Sandwich FLISA with peptide – peptide pair	peptide	-	1 × 10^{4} $TCID_{50}$/mL
Ref [162]	Polydimethylsiloxane based microfluidic device	Thiolated aptamers	-	1 pM
Ref [163]	Colorimetric analysis	Aptamers CFA0334	-	1 ×10^{5} pfu live Zika virus
Ref [164]	Direct ELISA	Cys-peptides	-	10^{5} copies/mL
Ref [165]	Peptide-based ELISA	Biotinylated 20 aa peptide	-	Direct ZIKV positive human sera at 1:800 – 1:100 dilution
Ref [166]	RT-LAMP combined LFA	ZIKV probe conjugated Au Nps	-	3 RNA copy number

observations demonstrate that when the gold salt composition is enhanced, the current and thus the electric charge increases, increasing the transducer's conductivity. SEM micrographs of GNPs electrodeposition from a 250 μM Au chloride.

VI. SUMMARY AND CONCLUSION

The COVID-19 pandemic has emphasized the urgent need to update clinical diagnostics and utilize innovative techniques for POC testing that are accurate and reliable. The COVID-19 pandemic has encouraged scientists to work on the formulation of a cutting-edge strategy that must be very competent and proficient in adjusting to the current demand for early detection in order to control this worldwide matter. As of recently no specific treatment for COVID-19 is available and due to the threat of new variants, the only way to control this pandemic is to detect, monitor, and prevent its infection in advance. Furthermore, the asymptomatic instances of COVID-19 have complicated the situation, necessitating the development of a fast and affordable technique for mass-scale initial detection of this infection in order to distinguish between infected and non-infected patients. In this review paper, we have discussed several recent developments in biosensors for the detection of COVID-19, Influenza, Ebola, and Zika virus both in terms of their principles of operation and the value they contribute to the virus's detection. We have discussed the recently developed electrochemical, electrochemical based microbiosensor, nanophotonic based, and protein based, field effect transistor based, boron-doped diamond based, label-free, DNA-based, and nanomaterial based biosensors for the rapid detection of SARS-CoV-2, Influenza, Ebola, and Zika viruses and the results are compared with the previously published work in terms of LOD, range of functionality and other important information. In terms of remarkable sensitivity, reduced size, and low cost, emerging sensors based on functional materials, nanotechnologies, and creative sensing processes exhibit potential. Novel intelligent sensing technologies that combine biosensors' ultrahigh sensitivity with artificial intelligence and the Internet of Things can aid in preventive measures. We strongly believe that these insights will aid in the study and development of a new generation of adaptable virus biosensors for fellow researchers.

REFERENCES

[1] Z. W. Ye, S. Yuan, K. S. Yuen, S. Y. Fung, C. P. Chan, and D. Y. Jin, "Zoonotic origins of human coronaviruses," International Journal of Biological Sciences, vol. 16, no. 10. pp. 1686–1697, 2020, doi: 10.7150/ijbs.45472.

[2] S. C. Weaver et al., "Zika virus: History, emergence, biology, and prospects for control," Antiviral Research, vol. 130. pp. 69–80, 2016, doi: 10.1016/j.antiviral.2016.03.010.

[3] J. Weyer, A. Grobbelaar, and L. Blumberg, "Ebola Virus Disease: History, Epidemiology and Outbreaks," Current Infectious Disease Reports, vol. 17, no. 5. pp. 1–8, 2015, doi: 10.1007/s11908-015-0480-y.

[4] G. W. A. Dick, "Zika Virus (I). Isolations and serological specificity," Trans. R. Soc. Trop. Med. Hyg., vol. 46, no. 5, pp. 509–520, 1952, doi: 10.1016/0035-9203(52)90042-4.

[5] F. N. MacNamara, "Zika virus: A report on three cases of human infection during an epidemic of jaundice in Nigeria," Trans. R. Soc. Trop. Med. Hyg., vol. 48, no. 2, pp. 139–145, 1954, doi: 10.1016/0035-9203(54)90006-1.

[6] J. Khubchandani, T. R. Jordan, and Y. T. Yang, "Ebola, zika, corona…what is next for our world?," International Journal of Environmental Research and Public Health, vol. 17, no. 9. 2020, doi: 10.3390/ijerph17093171.

[7] D. X. Liu, J. Q. Liang, and T. S. Fung, "Human Coronavirus-229E, -OC43, -NL63, and -HKU1 (Coronaviridae)," in Encyclopedia of Virology, 2021, pp. 428–440.

[8] A. M. Zaki, S. van Boheemen, T. M. Bestebroer, A. D. M. E. Osterhaus, and R. A. M. Fouchier, "Isolation of a Novel Coronavirus from a Man with Pneumonia in Saudi Arabia," N. Engl. J. Med., vol. 367, no 19, pp. 1814–1820, 2012, doi: 10.1056/nejmoa1211721.

[9] S. V. Vemula, J. Zhao, J. Liu, X. W. Xue, S. Biswas, and I. Hewlett, "Current approaches for diagnosis of influenza virus infections in humans," Viruses, vol. 8, no. 4. 2016, doi: 10.3390/v8040096.

[10] T. Ganzenmueller et al., "Comparison of the performance of direct fluorescent antibody staining, a point-of-care rapid antigen test and virus isolation with that of RT-PCR for the detection of novel 2009 influenza A (H1N1) virus in respiratory specimens," J. Med. Microbiol., vol. 59, no. 6, pp. 713–717, 2010, doi: 10.1099/jmm.0.017244-0.

[11] S. Vasoo, J. Stevens, and K. Singh, "Rapid antigen tests for diagnosis of pandemic (Swine) influenza A/H1N1," Clin. Infect. Dis., vol. 49, no. 7, pp. 1090–1093, 2009, doi: 10.1086/644743.

[12] S. Ng et al., "Novel correlates of protection against pandemic H1N1 influenza A virus infection," Nat. Med., vol. 25, no. 6, pp. 962–967, 2019, doi: 10.1038/s41591-019-0463-x.

[13] S. Dayakar, H. R. Pillai, V. P. Thulasi, D. Jayalekshmi, and R. R. Nair, "Comparative Study of Molecular Approaches for the Detection of Influenza Virus from Patient Samples Using Real-time PCR: Prospective Disease Burden Study in Kerala (India) from 2010 to 2016," Current Infectious Disease Reports, vol. 20, no. 8. 2018, doi: 10.1007/s11908-018-0632-y.

[14] S. Spencer, M. G. Thompson, B. Flannery, and A. Fry, "Comparison of respiratory specimen collection methods for detection of influenza virus infection by reverse transcription-PCR: A literature review," J. Clin. Microbiol., vol. 57, no. 9, 2019, doi: 10.1128/JCM.00027-19.

[15] P. Cherpillod et al., "Ebola virus disease diagnosis by real-time RT-PCR: A comparative study of 11 different procedures," J. Clin. Virol., vol. 77, pp. 9–14, 2016, doi: 10.1016/j.jcv.2016.01.017.

[16] M. Moreau et al., "Lactating mothers infected with Ebola virus: EBOV RTPCR of blood only may be insufficient," Eurosurveillance, vol. 20, no. 3, 2015, doi: 10.2807/1560-7917.ES2015.20.3.21017.

[17] F. Cui and H. S. Zhou, "Diagnostic methods and potential portable biosensors for coronavirus disease 2019," Biosens. Bioelectron., vol. 165, 2020, doi: 10.1016/j.bios.2020.112349.

[18] J. Yoon, H. Y. Cho, M. Shin, H. K. Choi, T. Lee, and J. W. Choi, "Flexible electrochemical biosensors for healthcare monitoring," Journal of Materials Chemistry B, vol. 8, no. 33. pp. 7303–7318, 2020, doi: 10.1039/d0tb01325k.

[19] S. Fruncillo, X. Su, H. Liu, and L. S. Wong, "Lithographic Processes for the Scalable Fabrication of Micro- And Nanostructures for Biochips and Biosensors," ACS Sensors, vol. 6, no. 6. 2021, doi: 10.1021/acssensors.0c02704.

[20] L. J. Carter et al., "Assay Techniques and Test Development for COVID-19 Diagnosis," ACS Cent. Sci., vol. 6, no. 5, pp. 591–605, 2020, doi: 10.1021/acscentsci.0c00501.

[21] C. Chartrand, N. Tremblay, C. Renaud, and J. Papenburg, "Diagnostic accuracy of rapid antigen detection tests for respiratory syncytial virus infection: Systematic review and meta-analysis," Journal of Clinical Microbiology, vol. 53, no. 12. pp. 3738–3749, 2015, doi: 10.1128/JCM.01816-15.

[22] E. Morales-Narváez and C. Dincer, "The impact of biosensing in a pandemic outbreak: COVID-19," Biosens. Bioelectron., vol. 163, 2020, doi: 10.1016/j.bios.2020.112274.

[23] T. K. N. Shobhit K Patel, Jaymit Surve, Juveriya Parmar, "Review on Graphene-based Absorbers for Infrared to Ultraviolet Frequencies," J. Adv. Eng. Comput., vol. 5, no. 4, pp. 214–238, 2021, doi: http://dx.doi.org/10.25073/jaec.202154.350.

[24] S. K. Patel, J. Parmar, J. Surve, S. Das, B. T. P. Madhav, and S. A. Taya, "Metamaterial-based refractive index sensor using Ge 2 Sb 2 Te 5 substrate for glucose detection," Microw. Opt. Technol. Lett., Mar. 2022, doi: 10.1002/mop.33204.

[25] S. B. Uzunoglu, T. Uzunoglu, S. Koçsuz, M. Evyapan, and O. Arslan, "Metal ion effects on Polyphenol Oxidase Covalently immobilized on a Bio-Composite," Cell. Mol. Biol., vol. 67, no. 2, pp. 50–55, 2021, doi: 10.14715/cmb/2021.67.2.8.

[26] S. Moradi, S. Khaledian, M. Abdoli, M. Shahlaei, and D. Kahrizi, "Nano-biosensors in cellular and molecular biology," Cell. Mol. Biol., vol. 64, no. 5, pp. 85–90, 2018, doi: 10.14715/cmb/2018.64.5.14.

[27] R. Lak, R. Yaghobi, and M. Garshasbi, "Importance of miR-125a-5p and miR-122-5p expression in patients with HBV infection," Cell. Mol. Biol., vol. 66, no. 5, pp. 1–8, 2020, doi: 10.14715/cmb/2020.66.5.1.

[28] S. T. J. Balaky et al., "A comprehensive review of histopathological findings of infections induced by COVID-19," Cellular and Molecular Biology, vol. 66, no. 7. pp. 143–151, 2020, doi: 10.14715/cmb/2020.66.7.22.

[29] L. Peng, F. Meng, Y. Liu, and L. Zhang, "Interleukin 8 Association with respiratory syncytial virus bronchiolitis: A systematic review and meta-analysis," Cell. Mol. Biol., vol. 66, no. 2, pp. 74–77, 2020, doi: 10.14715/cmb/2020.66.2.12.

[30] World Health Organization, "Novel Coronavirus (2019-nCoV) WHO Bulletin Situation Report - 1," World Heal. Organ., vol. 10, no. January, pp. 1–5, 2020.

[31] F. Wu et al., "A new coronavirus associated with human respiratory disease in China," Nature, vol. 579, no. 7798, pp. 265–269, 2020, doi: 10.1038/s41586-020-2008-3.

[32] A. E. Gorbalenya et al., "The species Severe acute respiratory syndrome-related coronavirus: classifying 2019-nCoV and naming it SARS-CoV-2," Nature Microbiology, vol. 5, no. 4. pp. 536–544, 2020, doi: 10.1038/s41564-020-0695-z.

[33] WHO, "World Health Organization. (2020). Coronavirus disease 2019 (COVID-19): situation report, 52. World Health Organization.," 2020.

[34] S. P. Kaur and V. Gupta, "COVID-19 Vaccine: A comprehensive status report," Virus Research, vol. 288. 2020, doi: 10.1016/j.virusres.2020.198114.

[35] WHO, "WHO Coronavirus (COVID-19) Dashboard," [Online]. Available: https://covid19.who.int/.

[36] S. M. H. Mahmud et al., "Bioinformatics and system biology approach to identify the influences of SARS-CoV-2 infections to idiopathic pulmonary fibrosis and chronic obstructive pulmonary disease patients," Brief. Bioinform., vol. 22, no. 5, 2021, doi: 10.1093/bib/bbab115.

[37] World Health Organization, "Tracking SARS-CoV-2 variants," Who, p. https://www.who.int/en/activities/tracking-SARS-Co, 2021, [Online]. Available: https://www.who.int/en/activities/tracking-SARS-CoV-2-variants/.

[38] E. Mostafavi, A. K. Dubey, L. Teodori, S. Ramakrishna, and A. Kaushik, "SARS-CoV-2 Omicron variant: A next phase of the COVID-19 pandemic and a call to arms for system sciences and precision medicine," MedComm, vol. 3, no. 1, Mar. 2022, doi: 10.1002/mco2.119.

[39] A. K. Kaushik and J. S. Dhau, "Photoelectrochemical oxidation assisted air purifiers; perspective as potential tools to control indoor SARS-CoV-2 Exposure," Appl. Surf. Sci. Adv., vol. 9, 2022, doi: 10.1016/j.apsadv.2022.100236.

[40] V. Chaudhary, A. Kaushik, H. Furukawa, and A. Khosla, "Review—Towards 5th Generation AI and IoT Driven Sustainable Intelligent Sensors Based on 2D MXenes and Borophene," ECS Sensors Plus, vol. 1, no. 1, p. 13601, 2022, doi: 10.1149/2754-2726/ac5ac6.

[41] S. K. Patel et al., "Encoding and tuning of THz metasurface-based refractive index sensor with behavior prediction using XGBoost Regressor," IEEE Access, pp. 1–1, 2022, doi: 10.1109/ACCESS.2022.3154386.

[42] S. K. Patel et al., "Graphene-based metasurface solar absorber design for the visible and near-infrared region with behavior prediction using Polynomial Regression," Optik (Stuttg)., p. 169298, May 2022, doi: 10.1016/j.ijleo.2022.169298.

[43] S. K. Patel, J. Surve, V. Katkar, and J. Parmar, "Optimization of Metamaterial-Based Solar Energy Absorber for Enhancing Solar Thermal Energy Conversion Using Artificial Intelligence," Adv. Theory Simulations, p. 2200139, May 2022, doi: 10.1002/adts.202200139.

[44] S. K. Patel, J. Surve, R. Jadeja, V. Katkar, J. Parmar, and K. Ahmed, "Ultra-Wideband, Polarization-Independent, Wide-Angle Multilayer Swastika-Shaped Metamaterial Solar Energy Absorber with Absorption Prediction using Machine Learning," Adv. Theory Simulations, p. 2100604, Feb. 2022, doi: 10.1002/adts.202100604.

[45] J. Parmar, S. K. Patel, V. Katkar, and A. Natesan, "Graphene-Based Refractive Index Sensor Using Machine Learning for Detection of Mycobacterium Tuberculosis Bacteria," IEEE Trans. Nanobioscience, pp. 1–1, 2022, doi: 10.1109/TNB.2022.3155264.

[46] S. Jain et al., "Internet of medical things (IoMT)-integrated biosensors for point-of-care testing of infectious diseases," Biosens. Bioelectron., vol. 179, 2021, doi: 10.1016/j.bios.2021.113074.

[47] A. K. Kaushik et al., "Electrochemical SARS-CoV-2 Sensing at Point-of-Care and Artificial Intelligence for Intelligent COVID-19 Management," ACS Applied Bio Materials. 2020, doi: 10.1021/acsabm.0c01004.

[48] S. Tiwari et al., "Antibacterial and antiviral high-performance nanosystems to mitigate new SARS-CoV-2 variants of concern," Current Opinion in Biomedical Engineering, vol. 21. 2022, doi: 10.1016/j.cobme.2021.100363.

[49] P. K. Sharma et al., "Ultrasensitive and Reusable Graphene Oxide-Modified Double-Interdigitated Capacitive (DIDC) Sensing Chip for Detecting SARS-CoV-2," ACS Sensors, 2021, doi: 10.1021/acssensors.1c01437.

[50] M. A. Mujawar, H. Gohel, S. K. Bhardwaj, S. Srinivasan, N. Hickman, and A. Kaushik, "Nano-enabled biosensing systems for intelligent healthcare: towards COVID-19 management," Materials Today Chemistry, vol. 17. 2020, doi: 10.1016/j.mtchem.2020.100306.

[51] A. Ahmadivand, B. Gerislioglu, Z. Ramezani, A. Kaushik, P. Manickam, and S. A. Ghoreishi, "Functionalized terahertz plasmonic metasensors: Femtomolar-level detection of SARS-CoV-2 spike proteins," Biosens. Bioelectron., vol. 177, 2021, doi: 10.1016/j.bios.2021.112971.

[52] T. A. Taz, K. Ahmed, B. K. Paul, F. A. Al-Zahrani, S. M. H. Mahmud, and M. A. Moni, "Identification of biomarkers and pathways for the SARS-CoV-2 infections that make complexities in pulmonary arterial hypertension patients," Brief. Bioinform., vol. 22, no. 2, pp. 1451–1465, 2021, doi: 10.1093/bib/bbab026.

[53] M. A. Zamzami et al., "Carbon nanotube field-effect transistor (CNT-FET)-based biosensor for rapid detection of SARS-CoV-2 (COVID-19) surface spike protein S1," Bioelectrochemistry, vol. 143, 2022, doi: 10.1016/j.bioelechem.2021.107982.

[54] W. A. El-Said and J. W. Choi, "Electrochemical Biosensor consisted of conducting polymer layer on gold nanodots patterned Indium Tin Oxide electrode for rapid and simultaneous determination of purine bases," Electrochim. Acta, vol. 123, pp. 51–57, 2014, doi: 10.1016/j.electacta.2013.12.144.

[55] M. Asad, A. Zulfiqar, R. Raza, M. Yang, A. Hayat, and N. Akhtar, "Orange Peel Derived C-dots Decorated CuO Nanorods for the Selective Monitoring of Dopamine from Deboned Chicken," Electroanalysis, vol. 32, no. 1, pp. 11–18, 2020, doi: 10.1002/elan.201900468.

[56] M. M. Khalifa et al., "Highly specific Electrochemical Sensing of Pseudomonas aeruginosa in patients suffering from corneal ulcers: A comparative study," Sci. Rep., vol. 9, no. 1, 2019, doi: 10.1038/s41598-019-54667-0.

[57] J. W. Shin, K. J. Kim, J. Yoon, J. Jo, W. A. El-Said, and J. W. Choi, "Silver nanoparticle modified electrode covered by graphene oxide for the enhanced electrochemical detection of dopamine," Sensors (Switzerland), vol. 17, no. 12, 2017, doi: 10.3390/s17122771.

[58] R. Li et al., "A flexible and physically transient electrochemical sensor for real-time wireless nitric oxide monitoring," Nat. Commun., vol. 11, no. 1, 2020, doi: 10.1038/s41467-020-17008-8.

[59] M. Senel, M. Dervisevic, M. Dervisevic, S. Alhassen, A. Alachkar, and N. H. Voelcker, "Electrochemical Micropyramid Array-Based Sensor for in Situ Monitoring of Dopamine Released from Neuroblastoma Cells," Anal. Chem., vol. 92, no. 11, pp. 7746–7753, 2020, doi: 10.1021/acs.analchem.0c00835.

[60] Y. Abbas et al., "Heteroatom-Doped Carbon Nanoparticle-Ionic Liquid Composites as Electrochemical Sensors for Uric Acid," ACS Appl. Nano Mater., vol. 3, no. 11, pp. 11383–11390, 2020, doi: 10.1021/acsanm.0c02466.

[61] W. A. El-Said et al., "Electrochemical Microbiosensor for Detecting COVID-19 in a Patient Sample Based on Gold Microcuboids Pattern," Biochip J., vol. 15, no. 3, pp. 287–295, 2021, doi: 10.1007/s13206-021-00030-3.

[62] G. Ruiz-Vega, M. Soler, and L. M. Lechuga, "Nanophotonic biosensors for point-of-care COVID-19 diagnostics and coronavirus surveillance," JPhys Photonics, vol. 3, no. 1. 2021, doi: 10.1088/2515-7647/abd4ee.

[63] A. B. González-Guerrero, J. Maldonado, S. Dante, D. Grajales, and L. M. Lechuga, "Direct and label-free detection of the human growth hormone in urine by an ultrasensitive bimodal waveguide biosensor," J. Biophotonics, vol. 10, no. 1, pp. 61–67, 2017, doi: 10.1002/jbio.201600154.

[64] J. Maldonado, M. C. Estévez, A. Fernández-Gavela, J. J. González-López, A. B. González-Guerrero, and L. M. Lechuga, "Label-free detection of nosocomial bacteria using a nanophotonic interferometric biosensor," Analyst, vol. 145, no. 2, pp. 497–506, 2020, doi: 10.1039/c9an01485c.

[65] C. S. Huertas, O. Calvo-Lozano, A. Mitchell, and L. M. Lechuga, "Advanced Evanescent-Wave Optical Biosensors for the Detection of Nucleic Acids: An Analytic Perspective," Frontiers in Chemistry, vol. 7. 2019, doi: 10.3389/fchem.2019.00724.

[66] D. Thomson et al., "Roadmap on silicon photonics," J. Opt. (United Kingdom), vol. 18, no. 7, 2016, doi: 10.1088/2040-8978/18/7/073003.

[67] V. V. Demidov, "Rolling-circle amplification in DNA diagnostics: The power of simplicity," Expert Review of Molecular Diagnostics, vol. 2, no. 6. pp. 542–548, 2002, doi: 10.1586/14737159.2.6.542.

[68] M. Shen et al., "Recent advances and perspectives of nucleic acid detection for coronavirus," Journal of Pharmaceutical Analysis, vol. 10, no. 2. pp. 97–101, 2020, doi: 10.1016/j.jpha.2020.02.010.

[69] T. Chaibun et al., "Rapid electrochemical detection of coronavirus SARS-CoV-2," Nat. Commun., vol. 12, no. 1, 2021, doi: 10.1038/s41467-021-21121-7.

[70] V. Stein and K. Alexandrov, "Synthetic protein switches: Design principles and applications," Trends in Biotechnology, vol. 33, no. 2. pp. 101–110, 2015, doi: 10.1016/j.tibtech.2014.11.010.

[71] A. Quijano-Rubio et al., "De novo design of modular and tunable protein biosensors," Nature, vol. 591, no. 7850, pp. 482–487, 2021, doi: 10.1038/s41586-021-03258-z.

[72] A. N. Baker et al., "The SARS-COV-2 Spike Protein Binds Sialic Acids and Enables Rapid Detection in a Lateral Flow Point of Care Diagnostic Device," ACS Cent. Sci., vol. 6, no. 11, pp. 2046–2052, 2020, doi: 10.1021/acscentsci.0c00855.

[73] P. Moitra et al., "Selective Naked-Eye Detection of SARS-CoV-2 Mediated by N Gene Targeted Antisense Oligonucleotide Capped Plasmonic Nanoparticles," ACS Nano, vol. 14, no. 6, pp. 7617–7627, 2020, doi: 10.1021/acsnano.0c03822.

[74] J. Jiao, C. Duan, L. Xue, Y. Liu, W. Sun, and Y. Xiang, "DNA nanoscaffold-based SARS-CoV-2 detection for COVID-19 diagnosis," Biosens. Bioelectron., vol. 167, 2020, doi: 10.1016/j.bios.2020.112479.

[75] G. Seo et al., "Rapid Detection of COVID-19 Causative Virus (SARS-CoV-2) in Human Nasopharyngeal Swab Specimens Using Field-Effect Transistor-Based Biosensor," ACS Nano, vol. 14, no. 4, pp. 5135–5142, 2020, doi: 10.1021/acsnano.0c02823.

[76] S. Mahari, A. Roberts, D. Shahdeo, and S. Gandhi, "Ecovsens-ultrasensitive novel in-house built printed circuit board based electrochemical device for rapid detection of nCovid-19 antigen, a spike protein domain 1 of SARS-CoV-2," bioRxiv, 2020, doi: 10.1101/2020.04.24.059204.

[77] V. Kumar et al., "Development of RNA-based assay for rapid detection of SARS-CoV-2 in clinical samples," bioRxiv, 2020, doi: 10.1101/2020.06.30.172833.

[78] X. Zhu et al., "Multiplex reverse transcription loop-mediated isothermal amplification combined with nanoparticle-based lateral flow biosensor for the diagnosis of COVID-19," Biosens. Bioelectron., vol. 166, 2020, doi: 10.1016/j.bios.2020.112437.

[79] Z. Zhao, H. Cui, W. Song, X. Ru, W. Zhou, and X. Yu, "A simple magnetic nanoparticles-based viral RNA extraction method for efficient detection of SARS-CoV-2," bioRxiv, 2020, doi: 10.1101/2020.02.22.961268.

[80] T. Lee et al., "Recent advances in AIV biosensors composed of nanobio hybrid material," Micromachines, vol. 9, no. 12. 2018, doi: 10.3390/mi9120651.

[81] Z. Huang et al., "Ultra-sensitive and high-throughput CRISPR-p owered COVID-19 diagnosis," Biosens. Bioelectron., vol. 164, 2020, doi: 10.1016/j.bios.2020.112316.

[82] J. P. Broughton et al., "CRISPR–Cas12-based detection of SARS-CoV-2," Nat. Biotechnol., vol. 38, no. 7, pp. 870–874, 2020, doi: 10.1038/s41587-020-0513-4.

[83] M. Patchsung et al., "Clinical validation of a Cas13-based assay for the detection of SARS-CoV-2 RNA," Nat. Biomed. Eng., vol. 4, no. 12, pp. 1140–1149, 2020, doi: 10.1038/s41551-020-00603-x.

[84] G. Qiu, Z. Gai, Y. Tao, J. Schmitt, G. A. Kullak-Ublick, and J. Wang, "Dual-Functional Plasmonic Photothermal Biosensors for Highly Accurate Severe Acute Respiratory Syndrome Coronavirus 2 Detection," ACS Nano, vol. 14, no. 5, pp. 5268–5277, 2020, doi: 10.1021/acsnano.0c02439.

[85] C. Yan et al., "Rapid and visual detection of 2019 novel coronavirus (SARS-CoV-2) by a reverse transcription loop-mediated isothermal amplification assay," Clin. Microbiol. Infect., vol. 26, no. 6, pp. 773–779, 2020, doi: 10.1016/j.cmi.2020.04.001.

[86] W. E. Huang et al., "RT-LAMP for rapid diagnosis of coronavirus SARS-CoV-2," Microb. Biotechnol., vol. 13, no. 4, pp. 950–961, 2020, doi: 10.1111/1751-7915.13586.

[87] Y. H. Baek et al., "Development of a reverse transcription-loop-mediated isothermal amplification as a rapid early-detection method for novel SARS-CoV-2," Emerg. Microbes Infect., vol. 9, no. 1, pp. 998–1007, 2020, doi: 10.1080/22221751.2020.1756698.

[88] B. Tian, F. Gao, J. Fock, M. Dufva, and M. F. Hansen, "Homogeneous circle-to-circle amplification for real-time optomagnetic detection of SARS-CoV-2 RdRp coding sequence," Biosens. Bioelectron., vol. 165, 2020, doi: 10.1016/j.bios.2020.112356.

[89] A. H. Reid, T. G. Fanning, J. V. Hultin, and J. K. Taubenberger, "Origin and evolution of the 1918 'Spanish' influenza virus hemagglutinin gene," Proc. Natl. Acad. Sci. U. S. A., vol. 96, no. 4, pp. 1651–1656, 1999, doi: 10.1073/pnas.96.4.1651.

[90] G. Neumann, T. Noda, and Y. Kawaoka, "Emergence and pandemic potential of swine-origin H1N1 influenza virus," Nature, vol. 459, no. 7249. pp. 931–939, 2009, doi: 10.1038/nature08157.

[91] U. Joseph et al., "Adaptation of Pandemic H2N2 Influenza A Viruses in Humans," J. Virol., vol. 89, no. 4, pp. 2442–2447, 2015, doi: 10.1128/jvi.02590-14.

[92] A. D. Iuliano et al., "Estimates of global seasonal influenza-associated respiratory mortality: a modelling study," Lancet, vol. 391, no. 10127, pp. 1285–1300, 2018, doi: 10.1016/S0140-6736(17)33293-2.

[93] E. C. J. Claas et al., "Human influenza A H5N1 virus related to a highly pathogenic avian influenza virus," Lancet, vol. 351, no. 9101, pp. 472–477, 1998, doi: 10.1016/S0140-6736(97)11212-0.

[94] R. Gao et al., "Human Infection with a Novel Avian-Origin Influenza A (H7N9) Virus," N. Engl. J. Med., vol. 368, no. 20, pp. 1888–1897, 2013, doi: 10.1056/nejmoa1304459.

[95] W. Song and K. Qin, "Human-infecting influenza A (H9N2) virus: A forgotten potential pandemic strain?," Zoonoses and Public Health, vol. 67, no. 3. pp. 203–212, 2020, doi: 10.1111/zph.12685.

[96] M. Okamatsu, T. Hiono, H. Kida, and Y. Sakoda, "Recent developments in the diagnosis of avian influenza," Veterinary Journal, vol. 215. pp. 82–86, 2016, doi: 10.1016/j.tvjl.2016.05.007.

[97] X. Xu et al., "Simultaneous detection of novel H7N9 and other influenza A viruses in poultry by multiplex real-time RT-PCR," Virol. J., vol. 12, no. 1, 2015, doi: 10.1186/s12985-015-0300-x.

[98] C. D. Ahberg, A. Manz, and P. Neuzil, "Single fluorescence channel-based multiplex detection of avian influenza virus by quantitative PCR with intercalating dye," Sci. Rep., vol. 5, 2015, doi: 10.1038/srep11479.

[99] J. Lee et al., "Evaluation of insulated isothermal PCR devices for the detection of avian influenza virus," J. Virol. Methods, vol. 292, 2021, doi: 10.1016/j.jviromet.2021.114126.

[100] H. Dhanze et al., "Seasonal Sero-prevalence of Japanese Encephalitis in Swine using Indirect IgG ELISA," J Vet Public Heal., vol. 12, no. 2, pp. 103–105, 2014.

[101] J. Fan et al., "Detection of a novel avian influenza A (H7N9) virus in humans by multiplex one-step real-time RT-PCR assay," BMC Infect. Dis., vol. 14, no. 1, 2014, doi: 10.1186/1471-2334-14-541.

[102] D. Nidzworski et al., "A rapid-response ultrasensitive biosensor for influenza virus detection using antibody modified boron-doped diamond," Sci. Rep., vol. 7, no. 1, 2017, doi: 10.1038/s41598-017-15806-7.

[103] J. A. Park et al., "Fabrication of electrochemical influenza virus (H1n1) biosensor composed of multifunctional dna four-way junction and molybdenum disulfide hybrid material," Materials (Basel)., vol. 14, no. 2, pp. 1–12, 2021, doi: 10.3390/ma14020343.

[104] H. Zhang, A. M. Klose, and B. L. Miller, "Label-Free, Multiplex Glycan Microarray Biosensor for Influenza Virus Detection," Bioconjug. Chem., vol. 32, no. 3, pp. 533–540, 2021, doi: 10.1021/acs.bioconjchem.0c00718.

[105] W. Weis, J. H. Brown, S. Cusack, J. C. Paulson, J. J. Skehel, and D. C. Wiley, "Structure of the influenza virus haemagglutinin complexed with its receptor, sialic acid," Nature, vol. 333, no. 6172, pp. 426–431, 1988, doi: 10.1038/333426a0.

[106] M. N. Matrosovich, T. Y. Matrosovich, T. Gray, N. A. Roberts, and H. D. Klenk, "Human and avian influenza viruses target different cell types in cultures of human airway epithelium," Proc. Natl. Acad. Sci. U. S. A., vol. 101, no. 13, pp. 4620–4624, 2004, doi: 10.1073/pnas.0308001101.

[107] K. Shinya, M. Ebina, S. Yamada, M. Ono, N. Kasai, and Y. Kawaoka, "Avian flu: influenza virus receptors in the human airway. SUPPLEMENTARY INFO," Nature, vol. 440, no. 7083, pp. 435–6, 2006, [Online]. Available: http://www.ncbi.nlm.nih.gov/pubmed/16554799.

[108] L. Byrd-Leotis et al., "Influenza binds phosphorylated glycans from human lung," Sci. Adv., vol. 5, no. 2, 2019, doi: 10.1126/sciadv.aav2554.

[109] Y. F. Chang et al., "Detection of swine-origin influenza A (H1N1) viruses using a localized surface plasmon coupled fluorescence fiber-optic biosensor," Biosens. Bioelectron., vol. 26, no. 3, pp. 1068–1073, 2010, doi: 10.1016/j.bios.2010.08.060.

[110] J. Zhang et al., "Protein-binding aptamer assisted signal amplification for the detection of influenza A (H1N1) DNA sequences based on quantum dot fluorescence polarization analysis," Analyst, vol. 138, no. 17, pp. 4722–4727, 2013, doi: 10.1039/c3an00830d.

[111] J. Bhardwaj, N. Chaudhary, H. Kim, and J. Jang, "Subtyping of influenza A H1N1 virus using a label-free electrochemical biosensor based on the DNA aptamer targeting the stem region of HA protein," Anal. Chim. Acta, vol. 1064, pp. 94–103, 2019, doi: 10.1016/j.aca.2019.03.005.

[112] N. Lee, C. Wang, and J. Park, "User-friendly point-of-care detection of influenza A (H1N1) virus using light guide in three-dimensional photonic crystal," RSC Adv., vol. 8, no. 41, pp. 22991–22997, 2018, doi: 10.1039/C8RA02596G.

[113] S. R. Ahmed, J. Kim, T. Suzuki, J. Lee, and E. Y. Park, "Detection of influenza virus using peroxidase-mimic of gold nanoparticles," Biotechnol. Bioeng., vol. 113, no. 10, pp. 2298–2303, 2016, doi: 10.1002/bit.25982.

[114] R. Singh, S. Hong, and J. Jang, "Label-free Detection of Influenza Viruses using a Reduced Graphene Oxide-based Electrochemical Immunosensor Integrated with a Microfluidic Platform," Sci. Rep., vol. 7, 2017, doi: 10.1038/srep42771.

[115] T. W. Owen, R. O. Al-Kaysi, C. J. Bardeen, and Q. Cheng, "Microgravimetric immunosensor for direct detection of aerosolized influenza A virus particles," Sensors Actuators, B Chem., vol. 126, no. 2, pp. 691–699, 2007, doi: 10.1016/j.snb.2007.04.028.

[116] T. M. Peduru Hewa, G. A. Tannock, D. E. Mainwaring, S. Harrison, and J. V. Fecondo, "The detection of influenza A and B viruses in clinical specimens using a quartz crystal microbalance," J. Virol. Methods, vol. 162, no. 1–2, pp. 14–21, 2009, doi: 10.1016/j.jviromet.2009.07.001.

[117] R. Wang et al., "Interdigitated array microelectrode based impedance immunosensor for detection of avian influenza virus H5N1," Talanta, vol. 79, no. 2, pp. 159–164, 2009, doi: 10.1016/j.talanta.2009.03.017.

[118] J. Lin et al., "A portable impedance biosensor instrument for rapid detection of avian influenza virus," in Proceedings of IEEE Sensors, 2010, pp. 1558–1563, doi: 10.1109/ICSENS.2010.5690302.

[119] D. Li et al., "A nanobeads amplified QCM immunosensor for the detection of avian influenza virus H5N1," Biosens. Bioelectron., vol. 26, no. 10, pp. 4146–4154, 2011, doi: 10.1016/j.bios.2011.04.010.

[120] T. Hampton, "Largest-ever outbreak of ebola virus disease thrusts experimental therapies, vaccines into spotlight," JAMA - J. Am. Med. Assoc., vol. 312, no. 10, pp. 987–989, 2014, doi: 10.1001/jama.2014.11170.

[121] A. MacNeil and P. E. Rollin, "Ebola and marburg hemorrhagic fevers: Neglected tropical diseases?," PLoS Negl. Trop. Dis., vol. 6, no. 6, 2012, doi: 10.1371/journal.pntd.0001546.

[122] C. P. Tseng and Y. J. Chan, "Overview of Ebola virus disease in 2014," Journal of the Chinese Medical Association, vol. 78, no. 1. pp. 51–55, 2015, doi: 10.1016/j.jcma.2014.11.007.

[123] "Ebola Virus Disease in West Africa — The First 9 Months of the Epidemic and Forward Projections," N. Engl. J. Med., vol. 371, no. 16, pp. 1481–1495, 2014, doi: 10.1056/nejmoa1411100.

[124] S. M. Bartsch, K. Gorham, and B. Y. Lee, "The cost of an ebola case," Pathog. Glob. Health, vol. 109, no. 1, pp. 4–9, 2015, doi: 10.1179/2047773214Y.0000000169.

[125] J. S. Schieffelin et al., "Clinical Illness and Outcomes in Patients with Ebola in Sierra Leone," N. Engl. J. Med., vol. 371, no. 22, pp. 2092–2100, 2014, doi: 10.1056/nejmoa1411680.

[126] E. M. Leroy et al., "Diagnosis of Ebola haemorrhagic fever by RT-PCR in an epidemic setting," J. Med. Virol., vol. 60, no. 4, pp. 463–467, 2000, doi: 10.1002/(SICI)1096-9071(200004)60:4¡463::AID-JMV15¿3.0.CO;2-M.

[127] D. S. Chertow, C. Kleine, J. K. Edwards, R. Scaini, R. Giuliani, and A. Sprecher, "Ebola Virus Disease in West Africa — Clinical Manifestations and Management," N. Engl. J. Med., vol. 371, no. 22, pp. 2054–2057, 2014, doi: 10.1056/nejmp1413084.

[128] J. T. Baca, V. Severns, D. Lovato, D. W. Branch, and R. S. Larson, "Rapid detection of Ebola virus with a reagent-free, point-of-care biosensor," Sensors (Switzerland), vol. 15, no. 4, pp. 8605–8614, 2015, doi: 10.3390/s150408605.

[129] J. S. Towner et al., "Rapid Diagnosis of Ebola Hemorrhagic Fever by Reverse Transcription-PCR in an Outbreak Setting and Assessment of Patient Viral Load as a Predictor of Outcome," J. Virol., vol. 78, no. 8, pp. 4330–4341, 2004, doi: 10.1128/jvi.78.8.4330-4341.2004.

[130] X. Sun et al., "Enzymatic amplification detection of peanut allergen Ara h1 using a stem-loop DNA biosensor modified with a chitosan-mutiwalled carbon nanotube nanocomposite and spongy gold film," Talanta, vol. 131, pp. 521–527, 2015, doi: 10.1016/j.talanta.2014.07.078.

[131] J. Tian, D. Wang, Y. Zheng, and T. Jing, "A high sensitive electrochemical avian influenza virus H7 biosensor based on CNTs/MoSx aerogel," Int. J. Electrochem. Sci., vol. 12, no. 4, pp. 2658–2668, 2017, doi: 10.20964/2017.04.30.

[132] A. Sonato et al., "A surface acoustic wave (SAW)-enhanced grating-coupling phase-interrogation surface plasmon resonance (SPR) microfluidic biosensor," Lab Chip, vol. 16, no. 7, pp. 1224–1233, 2016, doi: 10.1039/c6lc00057f.

[133] E. Gosselin, J. J. Vanden Eynde, A. Petit, J. Conti, and J. De Coninck, "Designing a high performance, stable spectroscopic biosensor for the binding of large and small molecules," J. Colloid Interface Sci., vol. 508, pp. 443–454, 2017, doi: 10.1016/j.jcis.2017.08.057.

[134] H. Ilkhani and S. Farhad, "A novel electrochemical DNA biosensor for Ebola virus detection," Anal. Biochem., vol. 557, pp. 151–155, 2018, doi: 10.1016/j.ab.2018.06.010.

[135] Y. Chen et al., "Field-Effect Transistor Biosensor for Rapid Detection of Ebola Antigen," Sci. Rep., vol. 7, no. 1, 2017, doi: 10.1038/s41598-017-11387-7.

[136] A. N. Abbas et al., "Black phosphorus gas sensors," ACS Nano, vol. 9, no. 5, pp. 5618–5624, 2015, doi: 10.1021/acsnano.5b01961.

[137] G. Zhou, J. Chang, S. Cui, H. Pu, Z. Wen, and J. Chen, "Real-time, selective detection of Pb2+ in water using a reduced graphene oxide/gold nanoparticle field-effect transistor device," ACS Appl. Mater. Interfaces, vol. 6, no. 21, pp. 19235–19241, 2014, doi: 10.1021/am505275a.

[138] D. Duan et al., "Nanozyme-strip for rapid local diagnosis of Ebola," Biosens. Bioelectron., vol. 74, pp. 134–141, 2015, doi: 10.1016/j.bios.2015.05.025.

[139] C. W. Yen et al., "Multicolored silver nanoparticles for multiplexed disease diagnostics: Distinguishing dengue, yellow fever, and Ebola viruses," Lab Chip, vol. 15, no. 7, pp. 1638–1641, 2015, doi: 10.1039/c5lc00055f.

[140] G. G. Daaboul, C. A. Lopez, J. Chinnala, B. B. Goldberg, J. H. Connor, and M. Selim Ünlü, "Digital sensing and sizing of vesicular

stomatitis virus pseudotypes in complex media: A model for ebola and marburg detection," ACS Nano, vol. 8, no. 6, pp. 6047–6055, 2014, doi: 10.1021/nn501312q.

[141] A. A. Yanik et al., "An optofluidic nanoplasmonic biosensor for direct detection of live viruses from biological media," Nano Lett., vol. 10, no. 12, pp. 4962–4969, 2010, doi: 10.1021/nl103025u.

[142] H. Cai et al., "Optofluidic analysis system for amplification-free, direct detection of Ebola infection," Sci. Rep., vol. 5, 2015, doi: 10.1038/srep14494.

[143] M. R. Duffy et al., "Zika Virus Outbreak on Yap Island, Federated States of Micronesia," N. Engl. J. Med., vol. 360, no. 24, pp. 2536–2543, 2009, doi: 10.1056/nejmoa0805715.

[144] V. M. Cao-Lormeau et al., "Zika virus, French Polynesia, South Pacific, 2013," Emerging Infectious Diseases, vol. 20, no. 6. pp. 1085–1086, 2014, doi: 10.3201/eid2006.140138.

[145] D. Musso et al., "Potential for Zika virus transmission through blood transfusion demonstrated during an outbreak in French Polynesia, November 2013 to February 2014," Eurosurveillance, vol. 19, no. 14, 2014, doi: 10.2807/1560-7917.ES2014.19.14.20761.

[146] M. Hennessey, M. Fischer, and J. E. Staples, "Zika Virus Spreads to New Areas - Region of the Americas, May 2015-January 2016," Am. J. Transplant., vol. 16, no. 3, pp. 1031–1034, 2016, doi: 10.1111/ajt.13743.

[147] C. A. Herrada, A. Kabir, R. Altamirano, and W. Asghar, "Advances in Diagnostic Methods for Zika Virus Infection," J. Med. Devices, Trans. ASME, vol. 12, no. 4, 2018, doi: 10.1115/1.4041086.

[148] L. Priyamvada et al., "Human antibody responses after dengue virus infection are highly cross-reactive to Zika virus," Proc. Natl. Acad. Sci. U. S. A., vol. 113, no. 28, pp. 7852–7857, 2016, doi: 10.1073/pnas.1607931113.

[149] A. T. V. Nguyen, B. T. Duong, H. Park, and S. J. Yeo, "Development of a peptide aptamer pair-linked rapid fluorescent diagnostic system for Zika virus detection," Biosens. Bioelectron., vol. 197, 2022, doi: 10.1016/j.bios.2021.113768.

[150] S. Cajigas, D. Alzate, and J. Orozco, "Gold nanoparticle/DNA-based nanobioconjugate for electrochemical detection of Zika virus," Microchim. Acta, vol. 187, no. 11, 2020, doi: 10.1007/s00604-020-04568-1.

[151] A. M. Dennis, J. B. Delehanty, and I. L. Medintz, "Emerging Physicochemical Phenomena along with New Opportunities at the Biomolecular-Nanoparticle Interface," Journal of Physical Chemistry Letters, vol. 7, no. 11. pp. 2139–2150, 2016, doi: 10.1021/acs.jpclett.6b00570.

[152] H. A. M. Faria and V. Zucolotto, "Label-free electrochemical DNA biosensor for zika virus identification," Biosens. Bioelectron., vol. 131, pp. 149–155, 2019, doi: 10.1016/j.bios.2019.02.018.

[153] A. C. R. Moço et al., "Electrochemical Detection of Zika Virus in Biological Samples: A Step for Diagnosis Point-of-care," Electroanalysis, vol. 31, no. 8, pp. 1597–1604, 2019, doi: 10.1002/elan.201900068.

[154] K. Takemura, O. Adegoke, T. Suzuki, and E. Y. Park, "A localized surface plasmon resonance-amplified immunofluorescence biosensor for ultrasensitive and rapid detection of nonstructural protein 1 of Zika virus," PLoS One, vol. 14, no. 1, 2019, doi: 10.1371/journal.pone.0211517.

[155] M. Steinmetz et al., "A sensitive label-free impedimetric DNA biosensor based on silsesquioxane-functionalized gold nanoparticles for Zika Virus detection," Biosens. Bioelectron., vol. 141, 2019, doi: 10.1016/j.bios.2019.111351.

[156] D. Alzate, S. Cajigas, S. Robledo, C. Muskus, and J. Orozco, "Genosensors for differential detection of Zika virus," Talanta, vol. 210, 2020, doi: 10.1016/j.talanta.2019.120648.

[157] A. Kaushik et al., "A sensitive electrochemical immunosensor for label-free detection of Zika-virus protein," Sci. Rep., vol. 8, no. 1, 2018, doi: 10.1038/s41598-018-28035-3.

[158] A. M. Faria and T. Mazon, "Early diagnosis of Zika infection using a ZnO nanostructures-based rapid electrochemical biosensor," Talanta, vol. 203, pp. 153–160, 2019, doi: 10.1016/j.talanta.2019.04.080.

[159] Q. Jiang, Y. J. Chandar, S. Cao, E. D. Kharasch, S. Singamaneni, and J. J. Morrissey, "Rapid, Point-of-Care, Paper-Based Plasmonic Biosensor for Zika Virus Diagnosis," Adv. Biosyst., vol. 1, no. 9, 2017, doi: 10.1002/adbi.201700096.

[160] K. H. Lee and H. Zeng, "Aptamer-Based ELISA Assay for Highly Specific and Sensitive Detection of Zika NS1 Protein," Anal. Chem., vol. 89, no. 23, pp. 12743–12748, 2017, doi: 10.1021/acs.analchem.7b02862.

[161] D. T. H. Kim, D. T. Bao, H. Park, N. M. Ngoc, and S. J. Yeo, "Development of a novel peptide aptamer-based immunoassay to detect Zika virus in serum and urine," Theranostics, vol. 8, no. 13, pp. 3629–3642, 2018, doi: 10.7150/thno.25955.

[162] N. Saraf, M. Villegas, B. J. Willenberg, and S. Seal, "Multiplex Viral Detection Platform Based on a Aptamers-Integrated Microfluidic Channel," ACS Omega, vol. 4, no. 1, pp. 2234–2240, 2019, doi: 10.1021/acsomega.8b03277.

[163] A. Bosak et al., "Aptamer-gold nanoparticle conjugates for the colorimetric detection of arboviruses and vector mosquito species," RSC Adv., vol. 9, no. 41, pp. 23752–23763, 2019, doi: 10.1039/c9ra02089f.

[164] M. Mascini et al., "Computationally designed peptides for zika virus detection: An incremental construction approach," Biomolecules, vol. 9, no. 9, 2019, doi: 10.3390/biom9090498.

[165] N. Mishra, R. Thakkar, J. Ng, and W. I. Lipkin, "Zika Virus Peptide ELISA (ZIKV-NS2B-Concat ELISA) for Detection of IgG Antibodies to Zika Virus Infection," in Methods in Molecular Biology, vol. 2142, 2020, pp. 113–122.

[166] G. Ahn et al., "Zika virus lateral flow assays using reverse transcription-loop-mediated isothermal amplification," RSC Adv., vol. 11, no. 29, pp. 17800–17808, 2021, doi: 10.1039/d1ra01227d.